RADC-TR-87-35
In-House Report
April 1987

INCREMENTAL DIFFRACTION COEFICIENTS FOR PLANAR SURFACES, PART I: THEORY

Robert A. Shore and Arthur D. Yaghjian

APPROVED FOR PUBLIC RELEASE; DISTRIBUTION UNLIMITED

ROME AIR DEVELOPMENT CENTER
Air Force Systems Command
Griffiss Air Force Base, NY 13441-5700

This report has been reviewed by the RADC Public Affairs Office (PA) and is releasable to the National Technical Information Service (NTIS). At NTIS it will be releasable to the general public, including foreign nations.

RADC-TR-87-35 has been reviewed and is approved for publication.

APPROVED:

J. LEON POIRIER
Chief, Applied Electromagnetics Division
Directorate of Electromagnetics

APPROVED:

ALLAN C. SCHELL
Director of Electromagnetics

FOR THE COMMANDER:

JOHN A. RITZ
Directorate of Plans & Programs

This report has been reviewed by the RADC Public Affairs Office (PA) and is releasable to the National Technical Information Service (NTIS). At NTIS it will be releasable to the general public, including foreign nations.

RADC-TR-87-35 has been reviewed and is approved for publication.

APPROVED: J Leon Poirier

J. LEON POIRIER
Chief, Applied Electromagnetics Division
Directorate of Electromagnetics

APPROVED: Allan C. Schell

ALLAN C. SCHELL
Director of Electromagnetics

FOR THE COMMANDER: John A. Ritz

JOHN A. RITZ
Directorate of Plans & Programs

Unclassified

SECURITY CLASSIFICATION OF THIS PAGE

REPORT DOCUMENTATION PAGE

Form Approved OMB No. 0704-0188

1a. REPORT SECURITY CLASSIFICATION Unclassified	1b. RESTRICTIVE MARKINGS
2a. SECURITY CLASSIFICATION AUTHORITY	3. DISTRIBUTION/AVAILABILITY OF REPORT Approved for Public Release; Distribution Unlimited
2b. DECLASSIFICATION/DOWNGRADING SCHEDULE	
4. PERFORMING ORGANIZATION REPORT NUMBER(S) RADC-TR-87-35	5. MONITORING ORGANIZATION REPORT NUMBER(S)
6a. NAME OF PERFORMING ORGANIZATION Rome Air Development Center 6b. OFFICE SYMBOL (If applicable) EECT	7a. NAME OF MONITORING ORGANIZATION
6c. ADDRESS (City, State, and ZIP Code) Hanscom AFB Massachusetts, 01731-5000	7b. ADDRESS (City, State, and ZIP Code)
8a. NAME OF FUNDING/SPONSORING ORGANIZATION 8b. OFFICE SYMBOL (If applicable)	9. PROCUREMENT INSTRUMENT IDENTIFICATION NUMBER
8c. ADDRESS (City, State, and ZIP Code)	10. SOURCE OF FUNDING NUMBERS PROGRAM ELEMENT NO.: 61102F PROJECT NO.: 2305 TASK NO.: J4 WORK UNIT ACCESSION NO.: 04

11. TITLE (Include Security Classification)

Incremental Diffraction Coefficients for Planar Surfaces, Part I: Theory

12. PERSONAL AUTHOR(S)

Shore, Robert A., and Yaghjian, Arthur D.

13a. TYPE OF REPORT	13b. TIME COVERED	14. DATE OF REPORT (Year, Month, Day)	15. PAGE COUNT
In-House	FROM 3/86 TO 12/86	1987 April	48

16. SUPPLEMENTARY NOTATION

17. COSATI CODES			18. SUBJECT TERMS (Continue on reverse if necessary and identify by block number)
FIELD	GROUP	SUB-GROUP	Diffraction coefficients
20	03	14	Incremental length

19. ABSTRACT (Continue on reverse if necessary and identify by block number)

Exact expressions for incremental diffraction coefficients at arbitrary angles of incidence and scattering are derived directly in terms of the corresponding two-dimensional, cylindrical diffraction coefficients. Specifically, if one can supply an expression for the conventional diffraction coefficients of a two-dimensional planar scatterer, one can immediately find the incremental diffraction coefficients through direct substitution. No integration, differentiation, or specific knowledge of the current is required. The derivation is limited to perfectly conducting scatterers that consist of planar surfaces, such as the wedge, the slit in an infinite plane, the strip, parallel or skewed planes, polygonal cylinders, or any combination thereof; and requires a known expression (whether exact or approximate) for the two-dimensional diffraction coefficients produced by the current on each different plane. Special attention is given to defining unambiguously all real angles and their analytic continuation into the imaginary values required by the incremental diffraction coefficients. (Cont.)

20. DISTRIBUTION/AVAILABILITY OF ABSTRACT ☒ UNCLASSIFIED/UNLIMITED ☐ SAME AS RPT. ☐ DTIC USERS	21. ABSTRACT SECURITY CLASSIFICATION Unclassified
22a. NAME OF RESPONSIBLE INDIVIDUAL Arthur D. Yaghjian	22b. TELEPHONE (Include Area Code) (617) 377-4329 22c. OFFICE SYMBOL RADC/EECT

DD Form 1473, JUN 86 Previous editions are obsolete.

SECURITY CLASSIFICATION OF THIS PAGE
Unclassified

Block 19 (cont.):

We confirm the validity of the general expressions by showing that the physical theory of diffraction, geometrical theory of diffraction, and physical optics incremental diffraction coefficients obtained by direct substitution into the general expressions agree with the results of Mitzner, Michaeli, and Knott, respectively, in the case of the infinite wedge. In addition, it is shown that the two-dimensional diffraction coefficients are recovered when the general expressions for the incremental diffraction coefficients are integrated over an infinite straight line. Finally, our general method is used to obtain, for the first time, the incremental diffraction coefficients for the infinitely long, narrow strip and slit.

Contents

Illustrations

Incremental Diffraction Coefficients for Planar Surfaces, Part 1: Theory

1. INTRODUCTION

Consider an electromagnetic wave in free space incident upon a perfectly conducting scatterer. To a first approximation, the surface current induced on the scatterer will be the physical optics (PO) current, that is, $2\hat{n} \times \bar{H}_i$ on the illuminated side of the scatterer and zero on the shadow side. To obtain the scattered fields radiated by the PO current, the PO current (multiplied by the free space Green's function) can usually be integrated numerically, sometimes analytically, and often asymptotically for certain regions of observation. In particular, a variety of computer programs exist for calculating the far fields of reflector antennas by integrating the PO current induced on the reflector by a given feed illumination.[1]

Of course, the scattered fields obtained from the PO current will not be exact unless the PO current equals the total surface current. Thus, the accuracy of the computed scattered fields can be improved if one can estimate the contribution to the scattered fields of the difference between the total and PO currents. Even for electrically large scatterers, this difference current or "nonuniform current,"† to use the terminology of Ufimtsev,[2,3] can strongly affect the scattered fields. For example, the far fields of the nonuniform current near the rims of reflectors can appreciably change the further-out side lobes of the copolarized fields and all the lobes of the cross-polarized fields.[4,5] In general, the inclusion of the fields radiated by the nonuniform currents is especially important for the accurate determination of cross-polarized fields, side-lobe fields, and fields near nulls.

If one does not know the exact solution to the scattering problem, one must approximate the nonuniform current. Ufimtsev,[2,3] in developing his "physical theory of diffraction" (PTD), assumes that the nonuniform current at a given point on a general electrically large scatterer is approximately equal to the nonuniform current of a corresponding canonical scatterer that conforms to the shape of the general scatterer in the locality of the given point. (The incident field for the canonical scatterer is also chosen as

(Received for publication 14 April 1987)

†Nonuniform currents near edges are commonly called "fringe currents."[27]

the incident field in the locality of the given point on the general scatterer.) For example, the nonuniform current near the rim of an illuminated thin-metal reflector would be approximated locally by the nonuniform current near the edge of a correspondingly illuminated, perfectly conducting half-plane. Similarly, the nonuniform current near the slits between panels that may form the reflector surface would be approximated by the nonuniform current near an infinite straight slit in an infinite perfectly conducting plane.

Typically, the predominant nonuniform currents vary rapidly over a transverse distance less than a wavelength. Moreover, closed-form expressions for the nonuniform currents of canonical problems are not generally available. Thus, unlike the PO current, it is usually impractical to numerically integrate the nonuniform currents on a general scatterer to obtain their radiated fields.

Fortunately, the far fields radiated by the nonuniform currents of a number of two-dimensional canonical problems can be expressed in closed form, even though the nonuniform currents themselves usually cannot. Specifically, the total diffracted far fields that result from plane-wave illumination are known in closed form for these canonical scatterers. In addition, the PO current for these scatterers under plane-wave illumination can usually be integrated to obtain closed-form expressions for the PO diffracted far fields. Thus, the far fields radiated by the nonuniform currents of these two-dimensional canonical problems can be found in closed form, simply by subtracting the PO far fields from the total far fields, since the nonuniform current is defined as the difference between the total and PO currents. Of course, this technique for finding the fields radiated by the nonuniform currents of canonical scatterers is precisely the one that Ufimtsev used to obtain closed-form expressions for the nonuniform or PTD diffraction coefficients for the perfectly conducting wedge.[2,3] Because the total diffracted fields define the coefficients of the geometrical theory of diffraction (GTD),[6,7] one is also correct in saying that Ufimtsev obtained the PTD diffraction coefficients by subtracting the PO diffraction coefficients from the GTD diffraction coefficients.†

Through an asymptotic analysis of the diffraction integral, Van Kampen[9,10] shows that the dominant high-frequency diffracted fields of a general three-dimensional scatterer emanate (or appear to emanate) from "critical points" on the scatterer where the ray path length becomes stationary or discontinuous (including discontinuities in derivatives of the path length). Van Kampen shows further that the critical points can be divided into critical points of the first, second, or third kind depending upon whether they are (1) stationary points on the surface of integration (specular reflection), (2) stationary points along a curve (edge, shadow, boundary, etc.) bounding the surface of integration, or (3) discontinuities (such as corners and tips) in the slope (or higher order derivatives) of a bounding curve.

When the frequency is high enough that several Fresnel zones are contained in a neighborhood of a critical point, and the amplitude of the incident field does not vary appreciably over this neighborhood, the diffracted field of this critical point is well approximated by the first term of the high-frequency asymptotic

†For two-dimensional canonical problems of infinite cross section, like the perfectly conducting wedge, the far fields of the total and PO current for an incident plane wave approach infinity at the shadow and reflection boundaries. Since the PO current is removed from the total current in the determination of the PTD diffraction coefficients, the PTD diffraction coefficients for such canonical problems have the advantage of the GTD coefficients of remaining finite at shadow and reflection boundaries, except for grazing incidence along an infinite face. The GTD coefficients, when applied to general scatterers, have the advantage over the PTD coefficients of not requiring a separate evaluation of the PO fields away from the shadow and reflection boundaries. The GTD singularities at the shadow and reflection boundaries are removed in "uniform geometrical theories of diffraction" that consider the source or field points at a finite distance from the scatterer. However, the shadow and reflection singularities remain a difficulty for GTD under scattering conditions most commonly encountered in practice, namely, large distances to the source and field points. Also, in the particular case of a plane H-wave illuminating a wedge, both the GTD and PTD diffraction coefficients are discontinuous across the faces of the wedge, as a function of either the incident angle or the scattering angle. In applying the wedge diffraction coefficients to general scatterers, these face-angle discontinuities can be removed, but only by ad hoc truncation of the current tails or by considering multiple interactions, if possible, between different parts of the scatterer.[8]

expansion.[9] Under these conditions, the three-dimensional diffracted fields from a critical point of the second kind lie on the local cone of diffraction and, therefore, can be expressed directly in terms of the diffraction coefficients of the two-dimensional canonical scatterer that conforms locally to the general scatterer at that point.[2,3,6,7] This powerful result, which combines the assumption that, at high frequencies, canonical currents approximate the local currents on the general scatterer, with the derivation of a generalized Fermat's principle, is the keystone and main reason for the success of both the physical and geometrical theories of diffraction. The approximation of local scattering by canonical scattering and the generalization of Fermat's principle are sometimes stated as the two fundamental postulates of the geometrical theory of diffraction.[11] However, only the assumption that high-frequency scattering is a local phenomenon that can be approximated by canonical scattering need be postulated, because, as discussed above, the generalization of Fermat's principle is derivable from an asymptotic treatment of the diffraction integral.[9,10]†

For critical points of the second kind that do not have several neighboring Fresnel zones, for example, observation points near caustics of the scattered field, or that have an incident field with an appreciable variation in amplitude along the curve near the critical point, and for critical points of the third kind, that is, points of abrupt change in smooth curves, the diffracted fields do not, in general, lie on isolated local cones of diffraction, and thus cannot be expressed directly in terms of the diffraction coefficients of the corresponding two-dimensional canonical problems. To remedy this deficiency, Mitzner introduced "incremental length diffraction coefficients"[17] that, when multiplied by the incident field, could be integrated along a bounding curve of the scatterer to obtain the diffracted fields of the nonuniform current for arbitrary angles of incidence and scattering.

The PTD incremental diffraction coefficients as defined by Mitzner give the far fields (in any direction) radiated by the nonuniform current on a differential length of an infinite cylinder of arbitrary cross section (two-dimensional canonical problem) illuminated by a plane wave at an arbitrary angle of incidence. Under the assumption that high-frequency diffraction is a local phenomenon, the fields radiated by each differential length of the nonuniform current on a general scatterer will be the same as the fields radiated by the differential length of the corresponding two-dimensional canonical scatterer. Thus, the scattered fields radiated by a general scatterer can be determined by integrating the appropriate incremental diffraction coefficients over the bounding curves of the scatterer. For example, a computer program that computes the fields of a reflector antenna by integrating the PO current can be improved to include the contribution from the nonuniform current by integrating the incremental diffraction coefficients (multiplied by the feed illumination) around the edge of the reflector and along the slits between the panels that form the reflector. Separate, ad hoc analyses to obtain the field in caustic (focal) regions, main beam and near-in side-lobe regions, or from corners (neglecting the higher-order distortion of the current near corners) become unnecessary. Once the computer program is fed the geometry of the scatterer and the incident field, the fields everywhere can be computed straightforwardly by two algorithms: one that integrates the PO current and one that integrates the incremental diffraction coefficients. Moreover, tangential slope and

---

†As early as 1902, Schwarzschild[12] presented the idea of using the canonical half-plane solution to obtain an improved solution to diffraction by a slit. However, the first paper to combine the idea of using canonical solutions wth a stationary phase evaluation that included edges (generalized Fermat's principle) is apparently the classic 1912 paper by MacDonald.[13,14] In 1950, Braunbek[15] developed further these two basic ideas of the modern theories of diffraction and applied them in detail to the circular aperture and disc. Both Ufimtsev[2] and Keller et al.[6] reference Braunbek,[15] who formulated a physical theory of diffraction by adding nonuniform "correction" fields to the uniform Kirchhoff fields in the aperture of a plane screen or on a disc. Although we concentrate on the Ufimtsev current formulation in the present paper, it is emphasized that similar results could be derived as well for a Braunbek field formulation. Such a formulation involving nonuniform correction near fields instead of nonuniform currents would apply conveniently to improving the accuracy of the radiated fields computed from a geometrical-optics aperture field integration.[1,16]

higher tangential derivative diffraction coefficients are computed implicitly when integrating the incremental diffraction coefficients multiplied by the incident field. (In the remainder of this report, we will sometimes loosely refer to "integration of incremental diffraction coefficients" without explicit mention that the coefficients are multiplied by the incident field.)

Of course, for curves that have only ordinary stationary points illuminated by incident fields with slowly varying amplitudes over several Fresnel zones, the integration should yield approximately the same values of the fields as those obtained wthout integration directly from the conventional two-dimensional diffraction coefficien^^. However, as mentioned above, integration of the incremental diffraction coefficients has the advantage of determining accurately the fields of the nonuniform current of a general scatterer for many geometries, observation angles, and incident fields for which the first order diffraction fields are a poor approximation; in addition, tangential slope or higher tangential derivative diffraction coefficients are not required when the variation in amplitude of the incident field becomes appreciable along the direction tangent to the curve. Also, the extra computer time required to integrate the incremental diffraction coefficients along bounding curves is generally small compared to the computer time required to do a two-dimensional integration of the PO current.

As with the conventional two-dimensional diffraction coefficients, incremental diffraction coefficients can be defined for the total current of cylinders to yield GTD incremental diffraction coefficients,[18] or for the PO current to yield PO incremental coefficients. The PTD (Mitzner) incremental diffraction coefficients can be obtained by subtracting the PO incremental diffraction coefficients from the GTD incremental diffraction coefficients.[19] The comparative advantages mentioned in the footnote on page 2 for PTD and GTD two-dimensional diffraction coefficients hold also for the incremental diffraction coefficients.

The implicit use of the concept of incremental diffraction coefficients was made in work that preceded that of Mitzner,[17] notably that of Ufimtsev,[2,3] Braunbek,[15] Millar,[20-22] and the "equivalent (edge) current work of Ryan and Peters.[23] However, this previous work required the fields of the incremental diffraction coefficients only near focal regions where slight, ad hoc modifications to the scattered fields along the diffraction cones were adequate. Knott and Senior[24] review the use of GTD "equivalent currents" before 1974 as well as extend the technique of Ryan and Peters to obtain approximate GTD incremental diffraction coefficients for arbitrary angles of incidence and scattering. In a 1985 publication,[33] Knott reviews further the subject of equivalent currents and incremental length diffraction coefficients.

To the authors' knowledge, exact expressions for the incremental diffraction coefficients have been found previously only for the perfectly conducting wedge. Mitzner[17] determined the PTD incremental diffraction coefficients of the wedge by matching the required nonuniform current integrals to similar integrals that occur for the two-dimensional wedge diffraction coefficients. Ten years later, Michaeli[18] determined the GTD incremental diffraction coefficients of the wedge by integrating the total wedge current in closed form.

The main objective of this report is to complement the work of Mitzner[17] and Michaeli[18] by providing a more general, convenient method for determining incremental diffraction coefficients. Specifically, we derive exact expressions for the incremental diffraction coefficients at arbitrary angles of incidence and scattering directly in terms of the corresponding two-dimensional diffraction coefficients. The derivation is limited to perfectly conducting scatterers that consist of planar surfaces, such as the wedge, the slit in an infinite plane, the strip, parallel or skewed planes, polygonal cylinde~ or any combination thereof. The derivation also requires a closed-form expression, whether exact or approximate, for the two-dimensional diffraction coefficients produced by the current on each different plane. In other words, if one can supply a closed-form expression for the conventional diffraction coefficients of a two-dimensional planar scatterer, one can immediately find the incremental diffraction coefficients through direct substitution. No integration, differentiation, nor specific knowledge of the current is required. (Also, the restriction to "closed-form" expressions can be removed for the many problems that require only real angles of the diffraction coefficients.)

We show that the PTD, GTD, and PO incremental diffraction coefficients obtained by direct substitution into the general expressions agree with the results of Mitzner,[17] Michaeli,[18,27] and Knott,[19,33] respectively, in the case of the infinite wedge. In addition, it is shown that the two-dimensional diffraction coefficients are recovered when the general expressions for the incremental diffraction coefficients are integrated over an infinite straight line. Finally, we use our general method to obtain for the first time the incremental diffraction coefficients for the infinitely long, narrow strip and slit.

In sequels (Parts II and III) to the present report, the incremental diffraction coefficients for the half plane and for the narrow slit are integrated around the rims of reflectors and along the slits between panels of the reflectors to obtain the far fields produced by the nonuniform currents. These computed far fields of the nonuniform current are added to the far fields computed from the PO current to improve the accuracy of the far fields especially, as mentioned above, in cross polarization, in the further-out side lobes, and near nulls.

2. FIELDS OF CURRENT PRODUCED BY A PLANE WAVE INCIDENT ON A TWO-DIMENSIONAL, PERFECTLY CONDUCTING SCATTERER

Figure 1 shows the surface current sheet on a planar facet of a two-dimensional, perfectly electrically conducting scatterer in free space. The scatterer extends uniformly to infinity in the $\pm z$ direction, and the planar facet lies in the xz plane. The scatterer is illuminated by a plane wave with propagation vector $\bar{k}$, whose direction is denoted by the spherical angles θ_o and ϕ_o. The magnitude of $\bar{k}$ equals $k = 2\pi/\lambda = \omega/c$, where λ is the free-space wavelength, ω is the angular frequency of the suppressed $\exp(-i\omega t)$ time dependence ($\omega > 0$), and c is the speed of light in free space.

Maxwell's equations and the boundary condition of zero tangential electric field on the perfectly electrically conducting scatterer show that, for plane-wave illumination, the surface current $\bar{\mathcal{K}}(\bar{r}')$ at any point $\bar{r}'$ on the current sheet can be factored as[35]

$$\bar{\mathcal{K}}(\bar{r}') = e^{-ikz'\cos\theta_o}\bar{K}(x'). \tag{1}$$

That is, the z'-dependence can be written explicitly in terms of the elevation angle θ_o of the incident plane wave, and thus, the remaining current factor $\bar{K}(x')$ depends on the transverse coordinate x', but not on the longitudinal coordinate z'. Although the phase of the z'-dependence in (1) is zero at $z' = 0$, (1) does not imply that the phase of the incident plane wave is zero at $z' = 0$ because an arbitrary constant phase factor can be implicitly contained in $\bar{K}(x')$. Of course, $\bar{K}(x')$ also depends implicitly on the angles (θ_o, ϕ_o) defining the direction of propagation of the incident plane wave, and is proportional to the complex amplitude of the incident plane wave. Also, the surface current described by (1) need not refer to the total current; in particular, it could refer to the PO current or the nonuniform current (total minus PO current).

2.1 Fields Produced by an Incremental Current Sheet

Let $\overline{dH}_s(\bar{r})$ be the scattered magnetic field at the point $\bar{r}$ radiated by the incremental current sheet of length dz'. (Initially, the axis of the incremental current sheet is chosen perpendicular to the z-axis; however, the analysis is generalized in Section 3.3 to allow the axis of the incremental current sheet to

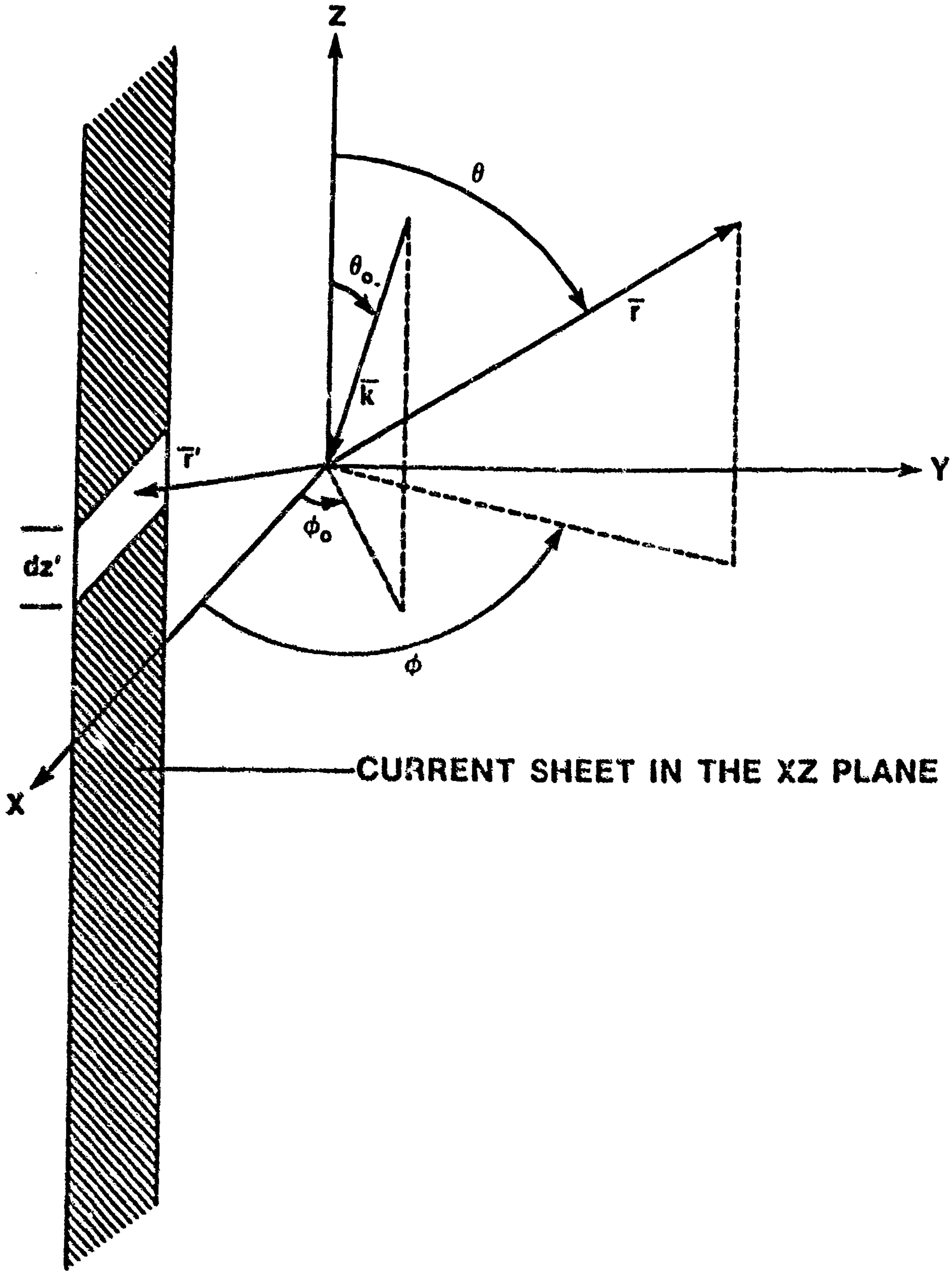

Figure 1 Planar Facet of a Two-Dimensional, Perfectly Conducting Scatterer in Free Space

make an arbitrary angle with the z-axis.) Through Maxwell's equations, we can express $\overline{dH}_s(\bar{r})$ in terms of the current by taking the curl of the vector potential:

$$\overline{dH}_s(\bar{r}) = \frac{dz'}{4\pi} e^{-ikz'\cos\theta_o} \nabla \times \int_{-\infty}^{\infty} \overline{K}(x') \frac{e^{ik|\bar{r}-\bar{r}'|}}{|\bar{r}-\bar{r}'|} dx'. \tag{2}$$

To obtain the magnetic far field from (2), take the limit as $r = |\bar{r}| \rightarrow \infty$, bring the limit under the integral,† and expand the scalar Green's function, $\exp(ik|\bar{r} - \bar{r}'|)/|\bar{r} - \bar{r}'|$, to get

$$\overline{dH}_s(\bar{r}) \underset{r\to\infty}{\sim} \frac{e^{ikr}dz'}{4\pi r} e^{-ikz'(\cos\theta+\cos\theta_o)} \cdot ik\hat{r} \times \int_{-\infty}^{\infty} \overline{K}(x') e^{-ikx'\sin\theta\cos\phi} dx'. \tag{3}$$

The spherical angles θ and ϕ define the direction of scattering, that is, the direction to the observation point $\bar{r}$ (see Figure 1), and the hat symbol ^ denotes unit vectors throughout. Although the limits of the x' integrations in (2) and (3) extend from $-\infty$ to ∞, they reduce to finite values for scatterers of finite transverse dimensions (like the one shown in Figure 1).

2.2 The Cylindrical Fields of the Current Sheet

The cylindrical fields of the entire current sheet in Figure 1 can be found by integrating (2) from $z' = -\infty$ to ∞. In the Appendix, we show that the z' integral can be expressed in closed form as

$$\int_{-\infty}^{\infty} e^{ikz'\cos\theta_0} \frac{e^{ik|\bar{r}-\bar{r}'|}}{|\bar{r}-\bar{r}'|} dz' = e^{-ikz\cos\theta_o} \pi i H_0^{(1)}(k \sin\theta_o |\bar{\rho} - x'\hat{x}|) \tag{4}$$

where $H_0^{(1)}$ is the Hankel function of the first kind, and $\bar{\rho}$ is the transverse part of $\bar{r}$, that is, $\bar{\rho} = \bar{r} - z\hat{z}$. Substitution of (4) into (2) integrated over z' gives the magnetic field $\overline{H}_s(\bar{r})$ of the entire current sheet as

$$\overline{H}_s(\bar{r}) = \frac{i}{4} \nabla \times e^{-ikz\cos\theta_o} \int_{-\infty}^{\infty} \overline{K}(x') H_0^{(1)} (k \sin\theta_o |\bar{\rho} - x'\hat{x}|) dx'. \tag{5}$$

To obtain the magnetic far field from (5) by taking the limit as $\rho \rightarrow \infty$, bring the limit under the integral (see footnote), and replace the Hankel function by its large-argument asymptotic form to get

$$\overline{H}_s(\bar{r}) \underset{\rho\to\infty}{\sim} \frac{e^{ik\hat{r}_o \cdot \bar{r}} e^{i\pi/4}}{(8\pi k\rho \sin\theta_o)^{1/2}} ik\hat{r}_o \times \int_{-\infty}^{\infty} \overline{K}(x') e^{-ikx'\sin\theta_o\cos\phi} dx'. \tag{6}$$

---

†At first sight, this interchange may not appear valid for scatterers with currents that extend to infinity in the transverse plane (such as the infinite wedge). However, the interchange can also be applied rigorously to these infinite scatterers by assuming that the currents have small exponential decay as $x' \rightarrow \pm \infty$.[26]

The unit vector $\hat{r}_o$ in (6) is defined as the unit vector $\hat{r}$ evaluated at $\theta = \pi - \theta_o$, that is, $\hat{r}_o = \hat{\rho}\sin\theta_o - \hat{z}\cos\theta_o$. Thus, we see that (6) represents a cylindrical wave propagating along the generators of the diffraction cone, that is, the scattered rays that make an angle θ with the longitudinal (z) axis equal to $\pi - \theta_o$.

For a number of canonical scatterers, the cylindrical far field given by (6) is known in closed form for the total current, PO current, and thus the nonuniform current. Consequently, the cross product of $\hat{r}_o$ and the current integral in (6) can be written in terms of these convenient closed-form canonical expressions. Moreover, in the next section, we show that the cross product of $\hat{r}$ and the current integral in (3) can be rewritten in terms of the cross product of $\hat{r}_o$ and the current integral in (6), so that the incremental far fields ($\overline{dH}_s$) can be written directly in terms of the canonical expressions for the cylindrical far fields ($\bar{H}_s$).

3. INCREMENTAL FAR FIELDS IN TERMS OF CYLINDRICAL FAR FIELDS

As a preliminary to expressing the incremental far fields in terms of the canonical cylindrical fields, let us rewrite (3) and (6) in the following form:

$$\overline{dH}_s(\bar{r}) \underset{r\to\infty}{\sim} dz' \frac{e^{ikr}\, ik}{4\pi r}\, \hat{r} \times \bar{A} = dz'\, C\hat{r} \times \bar{A} \tag{7}$$

$$\bar{H}_s(\bar{r}) \underset{r\to\infty}{\sim} \frac{e^{i\pi/4}\, e^{ik\hat{r}_o\cdot\bar{r}}\, ik}{(8\pi k\rho \sin\theta_o)^{1/2}}\, \hat{r}_o \times \bar{A}_o = C_o\hat{r}_o \times \bar{A}_o \tag{8}$$

where the vectors $\bar{A}$ and $\bar{A}_o$ are the current integrals in (3) and (6), respectively, that is,

$$\bar{A} = \int_{-\infty}^{\infty} \bar{K}(x')e^{-ikx'\sin\theta\cos\phi}\, dx' \tag{9a}$$

$$\bar{A}_o = \int_{-\infty}^{\infty} \bar{K}(x')e^{-ikx'\sin\theta_o\cos\phi}\, dx'. \tag{9b}$$

The constants C and C_o are defined by inspection of (7) and (8):

$$C = \frac{e^{ikr}\, ik}{4\pi r} \tag{10a}$$

$$C_o = \frac{e^{i\pi/4}\, e^{ik\hat{r}_o\cdot\bar{r}}\, ik}{(8\pi k\rho \sin\theta_o)^{1/2}} \tag{10b}$$

{The $\exp[-ikz'(\cos\theta + \cos\theta_o)]$ phase factor in (3) is eliminated in (7) by choosing the incremental current sheet at $z' = 0$.} Since the current sheet is in the xz-plane, K_y is zero and (7) and (8) can be written in terms of the x- and z-components of $\bar{A}$ and $\bar{A}_o$, respectively. Specifically, (7) and (8) become

$$\overline{dH}_s(\bar{r}) \underset{r\to\infty}{\sim} dz'\, C[A_x \sin\phi\hat{\theta} + (A_x \cos\theta \cos\phi - A_z \sin\theta)\hat{\phi}] \tag{11}$$

$$\overline{H}_s(\bar{r}) \underset{r\to\infty}{\sim} C_o[A_{ox} \sin\phi\, \hat{\theta}_o^{\pi} - (A_{ox} \cos\theta_o \cos\phi + A_{oz} \sin\theta_o)\hat{\phi}]. \tag{12}$$

The unit vectors $\hat{\theta}$ and $\hat{\phi}$ are retained in (11) and (12) because far fields conveniently polarize into θ and ϕ spherical components. The unit vector $\hat{\theta}_o^{\pi}$ in (12) denotes the unit vector $\hat{\theta}$ evaluated at the diffraction-cone angle $\theta = \pi - \theta_o$.

We are assuming a known expression for the θ- and ϕ- components of the far fields $\overline{H}_s(\bar{r})$ of the canonical current sheet. In other words, we are given $H_{s\theta}$ and $H_{s\phi}$ such that

$$\overline{H}_s(\bar{r}) \underset{r\to\infty}{\sim} H_{s\theta}\, \hat{\theta}_o^{\pi} + H_{s\phi}\, \hat{\phi}. \tag{13a}$$

We could, of course, just as well be given the far electric field $\overline{E}_s(\bar{r})$, which is related to $\overline{H}_s(\bar{r})$ by the cylindrical far-field formula

$$\overline{E}_s(\bar{r}) \sim -Z_o\hat{r}_o \times \overline{H}_s \sim -Z_o(H_{s\theta}\, \hat{\phi} - H_{s\phi}\, \hat{\theta}_o^{\pi}) \sim E_{s\phi}\, \hat{\phi} + E_{s\theta}\, \hat{\theta}_o^{\pi},\ r\to\infty \tag{13b}$$

in which Z_o is the impedance of free space. Equating the right sides of (12) and (13a) determines the rectangular components of $\bar{A}_o$ in terms of the given θ- and ϕ-components of $\overline{H}_s$:

$$A_{ox} = \frac{H_{s\theta}}{C_o \sin\phi} \tag{14a}$$

$$A_{oz} = \frac{-1}{C_o}\left(H_{s\theta} \cot\theta_o \cot\phi + \frac{H_{s\phi}}{\sin\theta_o}\right). \tag{14b}$$

Thus, the problem of finding the incremental far fields in terms of the canonical far fields reduces to finding A_x and A_z in (11) in terms of A_{ox} and A_{oz}, because A_{ox} and A_{oz} are known through (14).

3.1 Determination of the Rectangular Components of $\bar{A}$ in Terms of $\bar{A}_o$

Inspection of (9b) reveals that the rectangular components of $\bar{A}_o$ are functions of ϕ only through the $\cos\phi$ in the exponential of the integrand, because the rectangular components of $\overline{K}(x')$ do not depend on ϕ or θ. Therefore, the rectangular components of $\bar{A}$ in (9a) can be obtained merely by replacing ϕ with $\cos^{-1}(\sin\theta \cos\phi/\sin\theta_o)$ in $\bar{A}_o$ of (9b). Specifically, we have from (9a) and (9b)

$$\bar{A}(\theta, \phi) = \bar{A}_o\left[\phi \to \cos^{-1}\left(\frac{\sin\theta \cos\phi}{\sin\theta_o}\right)\right]. \tag{15}$$

(A similar substitution was used by Mitzner in Section 3.2.1 of Ref. 17 for the special case of the wedge.) Furthermore, the rectangular components of $\bar{A}$ can be related to the given components of the canonical cylindrical far fields by substituting A_{ox} and A_{oz} of (14) into (15) to get

$$A_x(\theta, \phi) = \frac{H_{s\theta}(\phi \to \cos^{-1} t)}{C_o \sin(\cos^{-1} t)} \tag{16a}$$

$$A_z(\theta, \phi) = -\frac{1}{C_o}\left[\frac{H_{s\theta}(\phi \to \cos^{-1} t)}{\sin(\cos^{-1} t)}\, t \cot\theta_o + \frac{H_{s\phi}(\phi \to \cos^{-1} t)}{\sin \theta_o}\right] \tag{16b}$$

where t stands for $\sin\theta \cos\phi/\sin\theta_o$. [Note from (10b) and the definition of $\hat{r}_o$ that C_o is not a function of ϕ.] Finally, insertion of A_x and A_z from (16) into (11) produces the desired expression for the incremental far fields as a direct function of the cylindrical far fields of the two-dimensional canonical scatterer:

$$\overline{dH}_s(\bar{r}) \sim dz' \frac{C}{C_o}\left\{\frac{H_{s\theta}(\phi \to \cos^{-1} t)}{\sin(\cos^{-1} t)}\sin\phi\hat{\theta} + \left[\frac{H_{s\theta}(\phi \to \cos^{-1} t)}{\sin(\cos^{-1} t)}(\cos\phi \cos\theta + t \sin\theta \cot\theta_o) + H_{s\phi}(\phi \to \cos^{-1} t)\frac{\sin\theta}{\sin\theta_o}\right]\hat{\phi}\right\} \tag{17}$$

where

$$\frac{C}{C_o} = \frac{e^{ikr}}{4\pi r}(8\pi k\rho \sin\theta_o)^{1/2} \exp\left[-i\left(k\rho \sin\theta_o - kz \cos\theta_o + \frac{\pi}{4}\right)\right],$$

and

$$t = \frac{\sin\theta \cos\phi}{\sin\theta_o}.$$

The far electric field $\overline{dE}_s$ of the incremental current is found from $\overline{dH}_s$ through the spherical far-field relationship

$$\overline{dE}_s \sim -Z_o \hat{r} \times \overline{dH}_s. \tag{18}$$

3.2 Evaluation of Incremental Far Fields for $|t| > 1$

The far fields radiated by an incremental current sheet can be found from (17) and (18) provided one knows the far fields of the corresponding two-dimensional canonical problem. Specifically, one must evaluate $H_{s\theta}$ and $H_{s\phi}$ for ϕ equal to $\cos^{-1}t$.

Although $\cos^{-1}t$ is a multiple-valued function, when it is substituted for ϕ in (9b), the unique value t is recovered. That is, A_{ox} and A_{oz}, and thus $H_{s\theta}/\sin(\cos^{-1}t)$ and $H_{s\phi}$ in (17) remain independent of which multiple value is chosen for $\cos^{-1}t$, as long as the same value is used throughout.

For $|t| < 1$, ϕ is a real angle and $H_{s\theta}$ and $H_{s\phi}$ can be evaluated from either numerical or closed-form expressions. However, for $|t| > 1$, ϕ is a complex angle, and thus, $H_{s\theta}$ and $H_{s\phi}$ must be evaluated outside their usual domain of scattering in real, physical space. This means that, if one merely has numerical values for $H_{s\theta}$ and $H_{s\phi}$ over the usual domain of $0 \le \phi < 2\pi$, one would not be able to determine their values directly for $|t| > 1$. †

Fortunately, (9b) shows that A_{ox} and A_{oz}, and thus $H_{s\theta}/\sin(\cos^{-1}t)$ and $H_{s\phi}$, are analytic functions of t for continuous†† currents $\bar{K}(x')$ that have *finite* extent in the x'-direction.[26] Therefore, if one has closed-form analytic expressions of $H_{s\theta}/\sin(\cos^{-1}t)$ and $H_{s\phi}$ for these finite problems solved originally for the domain $|t| < 1$, the same expressions can be used directly in the domain $|t| > 1$ as well. For a current sheet that extends to infinity along the x'-axis, such as the current on the face of the perfectly conducting wedge, the integral of (9b) is also an analytic function of t on the real axis, provided a small negative or positive imaginary part is added to t that produces an exponentially decaying integrand for x' integration that extends to plus or minus infinity, respectively.[26] Thus, for current sheets of infinite transverse extent, the closed-form expressions of $H_{s\theta}/\sin(\cos^{-1}t)$ and $H_{s\phi}$ in the domain $|t| < 1$ can also be evaluated by direct substitution of t (with a small loss approaching zero, if needed, to ensure analyticity over the entire real axis) in the domain $|t| > 1$. (The theorems on analyticity of integrals with finite limits [26] assure that the singularities of $1/\sin(\cos^{-1}t)$ in (17) at $t = \pm 1$ will be cancelled by zeros of $H_{s\theta}$ at $t = \pm 1$. These singularities may remain, however, for infinite current sheets, if a small imaginary part is not added to t.)

In summary, if closed-form expressions for the cylindrical far fields, $H_{s\theta}$ and $H_{s\phi}$, of the two-dimensional canonical scatterer are available over the usual domain of $|t| < 1$, these closed-form expressions can be used directly and unambiguously for all t to find the incremental far fields from (17) and (18). Of course, for normal incidence ($\theta_0 = \pi/2$), $|t|$ never exceeds one.

3.3 Singularities in the Incremental Far Fields

Singularities in the incremental far fields given by (17) and (18) will occur only at angles (θ, ϕ) where $H_{s\theta}(\phi \to \cos^{-1}t)/\sin(\cos^{-1}t)$ or $H_{s\phi}(\phi \to \cos^{-1}t)$ are singular. For canonical scatterers of finite transverse dimensions, integrability of the current in (9b) demands that these two functions be finite for all t, and thus, the incremental fields of finite canonical scatterers will have no singularities for all (θ, ϕ).

For infinite sheets of current like the total currents on the faces of the wedge, the cylindrical far-field functions $H_{s\theta}/\sin\phi$ and $H_{s\phi}$ have singularities at isolated values of azimuth angle ϕ for which the current integral in (9b) becomes infinite. Denoting these singular angles by ϕ_n, we see from (17) that the corresponding incremental far fields will, in general,††† have singularities for all θ and ϕ that satisfy $t = \cos\phi_n$, that is,

---

†Of course, if the current $\bar{K}(x')$ were known, one could conceivably integrate (9a) numerically or possibly analytically to obtain the A_x and A_z required to determine the incremental far fields immediately from (11). In fact, as mentioned in the Introduction, Michaeli[18] was able to perform the current integration in (9a) analytically for the faces of the perfectly conducting wedge to obtain the GTD incremental fields of the wedge. In the present paper, we want to avoid such involved current integrations by working directly with the cylindrical far fields of the corresponding two-dimensional canonical scatterers.

††For scatterers with sharp edges, the current may be singular at the edge. However, since these singularities are integrable, they can be removed from the integration by moving the limit of the integration just inside the edge, and thus, the theorems of Whittaker and Watson[26] still apply.

†††A notable exception can occur when $\theta_0 = \pi/2$, $\phi_n = 0$ so that (19) is satisfied only by the single far-field point $\theta = \pi/2$, $\phi = 0$ where the $\sin\phi$ and $(\cos\phi \cos\theta + t \sin\theta\cot\theta_0)$ factors in the numerators of (17) cancel the $\sin(\cos^{-1}t)$ factors in the denominators of (17). This exception is a particular example of the generalization (discussed later in Section 3.3) to current increments lying along the direction of the grazing diffracted ray.

$$\sin\theta \cos\phi = \sin\theta_o \cos\phi_n. \tag{19}$$

Eq. (19) defines a cone of far-field singularities in the incremental fields about the x-axis, that is, about the transverse coordinate axis of the current sheet. (This cone of singularities is not to be confused with the far-field cone of diffraction for the cylindrical fields about the z-axis, that is, the longitudinal axis of the planar current sheet.) The half angle α_n of the cone of singularities measured from the positive x-axis is given by

$$\alpha_n = \cos^{-1}(\cos\phi_n \sin\theta_o). \tag{20}$$

For normal incidence, θ_o equals $\pi/2$ and α_n equals ϕ_n. Geometrically, the cone of the far-field singularities of the incremental fields is generated by rotating about the x- axis the ray that lies in the direction of the singularity of the cylindrical far-field function ($H_{s\theta}/\sin\phi$ or $H_{s\phi}$). This generating ray, of course, lies on the cone of diffraction of the cylindrical far fields as well.

The total current on the illuminated face of a wedge has two associated cones of singularities given by (19). One is generated by the singularity in the diffracted fields at the shadow or reflection boundary ($\phi_n = \pi \pm \phi_o$), that is, the singularity produced by integration of the PO current in (9b). The second is generated by the singularity of $H_{s\theta}/\sin\phi$ (or $H_{s\phi}$ for a TM plane wave grazing at $\phi_o = \pi$) in the plane of the face ($\phi_n = 0, 2\pi$), that is, the singularity produced by integration of the nonuniform current in (9b) excited by an incident TE plane wave (or TM plane wave grazing at $\phi_o = \pi$). Both diffracted components, $H_{s\phi}$ and $H_{s\theta}/\sin\phi$, produced by the PO current remain finite at a face angle of the wedge (except for grazing incidence at $\phi_o = \pi$), whereas these same components produced by the nonuniform current remain finite at the shadow and reflection boundaries (except for grazing incidence at $\phi_o = \pi$). Therefore, in calculating the far fields of three-dimensional scattering bodies locally approximated by infinite two-dimensional canonical scatterers, like the wedge, with cylindrical far fields containing singularities at the shadow and reflection boundaries, it is especially advantageous to use the incremental far fields of the nonuniform (PTD) currents of the canonical scatterers, because the far fields of the nonuniform currents of these infinite scatterers do not contain singularities at the shadow and reflection boundaries, unlike the far fields of the total (GTD) and PO currents of these infinite scatterers. Moreover, in the PTD formulation, there are no singularities in the PO far fields if they are obtained by integrating numerically the PO current on the finite three-dimensional scatterer.

The cone of singularities defined by (19) that may occur at $\phi_n = 0, 2\pi$ for canonical scatterers of infinite transverse extent can be collapsed to a single line and sometimes eliminated by choosing the axis of the increment of current sheet skewed rather than perpendicular to the z-axis. In particular, Michaeli[27] has recently shown that the cone of singularities generated by the diffracted ray grazing the face of a wedge ($\phi_n = 0, 2\pi$) can be eliminated (except when the direction of incidence is also grazing at $\phi_o = \pi$) by choosing the axis of the incremental length in the direction of the grazing diffracted ray, that is, in the direction of propagation of the nonuniform current far from the edge. Butorin and Ufimtsev[37] derive the same result for scalar (acoustic) diffraction from the wedge.

The present analysis shows that choosing the positive x' integration axis of the incremental current sheet to make an arbitrary angle ψ with the positive z-axis (rather than 90°, as shown in Figure 1) multiplies the current in (3) by $\exp(-ikx' \cos\theta_o \cot\psi)$ and the exponential in the integrand of (3) by $\exp(-ikx' \cos\theta \cot\psi)$; thereby changing the integral on the right side of (3) to

$$\int_{-\infty}^{\infty} \overline{K}(x')\, e^{-ikx'[\sin\theta\cos\phi + \cot\psi\,(\cos\theta + \cos\theta_o)]}dx' \tag{21}$$

Thus, our general analysis and final results (17) and (18) for the incremental far fields remain the same when the axis of the incremental current sheet is skewed, except that t is set equal to t_ψ,

$$t_\psi = \left[\frac{\sin\theta\cos\phi + \cot\psi\,(\cos\theta + \cos\theta_o)}{\sin\theta_o}\right] \tag{22}$$

instead of to $\sin\theta\cos\phi/\sin\theta_o$. Eq. (22) reduces to Michaeli's corresponding result[27] for the faces of the infinite wedge when ψ is set equal to $\pi - \theta_o$, the angle of the grazing diffracted ray for a face along the positive x-axis. In that case, as mentioned above, the original singularity of the incremental diffracted fields at $\phi_n = 0, 2\pi$ is eliminated (except for grazing incidence at $\phi_o = \pi$) by substituting t_ψ for t; note, $t_\psi \leq 1$ for $\psi = \pi - \theta_o$. For a face extending to infinity along the negative x-axis, the angle of grazing is $\psi = \theta_o$, and the singularity at $t = -1$ is eliminated; note, $t_\psi \geq -1$ for $\psi = \theta_o$.

In summary, the differential increment of current on the face of a wedge forms a semi-infinite line source along the x-axis of Figure 1, and thus radiates with a symmetric vector potential about the x-axis. The total current of the line source can be divided into the PO current and the nonuniform current. The PO current of the line source radiates a far field that becomes singular in a cone of directions that includes the shadow and reflection directions of the corresponding two-dimensonal wedge face. The nonuniform current of the line source radiates a far field that becomes singular in a cone of directions that includes the diffracted ray along the corresponding two-dimensional wedge face. Skewing the axis of the differential increment of current to form a line source in the direction of the grazing diffracted ray rather than the x-axis collapses the cone of singularities of the nonuniform current to a single line in the direction of the grazing diffracted ray.

Skewing the axis of the current strip cannot eliminate the GTD and PO cone of singularities associated with the shadow and reflection boundaries ($\phi_n = \pi \pm \phi_o$) of the face of a wedge because for nongrazing incidence, the shadow and reflection boundaries of a face of a wedge do not lie along that face. Also, the directions of propagation of the PO and nonuniform currents on the face of a wedge are different except for normal ($\theta_o = \pi/2$) incidence or grazing incidence at $\phi_o = \pi$. Of course, the singularites in the PO far fields at the shadow and reflection boundaries of the infinite wedge can be eliminated by giving the faces of the wedge finite radii of curvature.[28] However, the resulting incremental diffraction coefficients apply then only to three-dimensional scatterers with curved rather than flat surfaces.

3.4 Division of Incremental Far Fields Into TE and TM Fields

The scattered fields of two-dimensional perfectly conducting cylinders divide conveniently into transverse electric (TE) and transverse magnetic (TM) fields depending on whether the incident plane wave is TE ($E_z = 0$) or TM ($H_z = 0$), respectively.[25]† Specifically, for the TE case, the far field component $H_{s\phi}$ is

†Although the diffracted fields radiated by the total currents of two-dimensional perfectly conducting cylinders divide conveniently into TE and TM fields, the fields radiated by the PO currents, and, thus, the fields radiated by the nonuniform currents do not divide generally into TE and TM fields, except for normal incidence ($\theta_o = 90°$). Consequently, (17) or (18) must be used, in general, rather than (23) or (24), to determine the incremental diffraction coefficients for the PO and nonuniform currents. (For example, see Section 4.3.)

zero everywhere (and, for the TM case, $H_{s\theta}$ is zero everywhere). Thus, the incremental magnetic far fields (17) for these TE and TM cylindrical fields reduce to

$$\overline{dH}_s^{TE}(\bar{r}) \underset{r\to\infty}{\sim} dz' \frac{CH_{s\theta}\,(\phi \to \cos^{-1} t)}{C_o \sin(\cos^{-1} t)} \; [\sin\phi\,\hat{\theta} + (\cos\phi\cos\theta + t\sin\theta\cot\theta_o)\,\hat{\phi}] \tag{23a}$$

$$\overline{dH}_s^{TM}(\bar{r}) \underset{r\to\infty}{\sim} dz' \frac{C}{C_o} H_{s\phi}\,(\phi \to \cos^{-1} t)\, \frac{\sin\theta}{\sin\theta_o}\,\hat{\phi}. \tag{23b}$$

The incremental electric far fields are obtained, as usual, from (18):

$$\overline{dE}_s^{TE}(\bar{r}) \underset{r\to\infty}{\sim} dz' \frac{CE_{s\phi}(\phi \to \cos^{-1} t)}{C_o \sin(\cos^{-1} t)} \; [\sin\phi\,\hat{\phi} - (\cos\phi\cos\theta + t\sin\theta\cot\theta_o)\,\hat{\theta}] \tag{24a}$$

$$\overline{dE}_s^{TM}(\bar{r}) \underset{r\to\infty}{\sim} dz' \frac{C}{C_o} E_{s\theta}\,(\phi \to \cos^{-1} t)\, \frac{\sin\theta}{\sin\theta_o}\,\hat{\theta} \tag{24b}$$

where $E_{s\phi}$ and $E_{s\theta}$, the cylindrical electric far fields, have been substituted from (13b). Note especially that the incremental TE magnetic and electric fields have both θ- and ϕ-components even though the corresponding TE cylindrical fields have only a θ-component of magnetic field and a ϕ-component of electric field. For the TM incremental magnetic or electric field, however, the single component of the corresponding TM cylindrical field remains as the only component. Recall that $E_{s\theta}$ and $H_{s\theta}$ as defined by (13) refer to the $\hat{\theta}_o^{\pi}$ components of the cylindrical far fields.

In dyadic notation, (24) can be written

$$\overline{dE}_s(\bar{r}) \underset{r\to\infty}{\sim} \bar{E}_s\,(\phi \to \cos^{-1} t) \cdot \bar{\bar{D}}_s\, dz' \tag{25}$$

where the components of the dyadic $\bar{\bar{D}}_s$ are the elements of the matrix defined by (24) that converts the cylindrical electric far field of the canonical scatterer to the corresponding incremental electric far field. If, in addition, we express the cylindrical electric far field as a dyadic $\bar{\bar{D}}$ multiplied by the incident field $\bar{E}_i$ (see, for example, Kouyoumjian[11]), that is,

$$\bar{E}_s = \bar{E}_i \cdot \bar{\bar{D}} \tag{26}$$

then (25) becomes

$$\overline{dE}_s(\bar{r}) \underset{r\to\infty}{\sim} \bar{E}_i \cdot (\bar{\bar{D}} \cdot \bar{\bar{D}}_s)dz' = \bar{E}_i \cdot \bar{\bar{D}}_I dz'. \tag{27}$$

[In (25), (26), and (27), we have included the radial dependence of the far fields in the dyadics.] The dyadic incremental diffraction coefficient $\bar{\bar{D}}_I$ provides an extremely compact notation (27) for the incremental diffraction fields. However, for detailed analytical or computational purposes, the explicit vector expressions (17), (18), (23), or (24) prove the more useful.

4. CHECKS ON THE CORRECTNESS OF THE EXPRESSIONS OBTAINED FOR THE INCREMENTAL FAR FIELD

In this section, we present a series of checks on the expressions that have been derived for the incremental far field. In Section 4.1, we integrate the incremental magnetic far field (17) from minus to plus infinity and show that, by doing so, we recover the cylindrical magnetic far field, (13a). In Section 4.2, we specialize our general results to the perfectly conducting half-plane and infinite wedge illuminated by a plane wave, obtain incremental far fields corresponding to both TM and TE incident illumination, and compare the resulting expressions with those obtained independently by Michaeli[18] through integration of the surface currents. Complete agreement is found between our expressions and his. In Section 4.3, we use our method to derive expressions for the incremental physical optics far field of a wedge illuminated by a plane wave. The resulting expressions for both TM and TE incident illumination are found to agree with those obtained independently by Knott[19,33] in his paper comparing the incremental diffraction coefficients of Michaeli[18] and Mitzner.[17]

4.1 Integration of the Incremental Far Field to Obtain the Cylindrical Far Field

A basic check on the expression (17) obtained for the incremental far field is that the integral of (17) over z' from minus to plus infinity should yield the cylindrical far field (13a). With the plan of evaluating the integral of (17) by the method of stationary phase, we write

$$\int_{-\infty}^{\infty} \overline{dH}_s(\bar{r}) = \int_{-\infty}^{\infty} e^{ik\rho q(z')}\bar{f}(z')\, dz' \tag{28}$$

where (see Figure 2)

$$\hat{r} = \bar{R} - z'\hat{z} \tag{29}$$

$$q(z') = \frac{1}{\rho}(r - z'\cos\theta_o) \tag{30}$$

and

$$\hat{f}(z') = \frac{(8\pi k\rho \sin\theta_o)^{1/2}}{4\pi r} e^{-ik\hat{r}_o \cdot \hat{R} - i\pi/4}$$

$$\cdot \left\{ \frac{H_{s\theta}(\phi \to \cos^{-1} t')}{\sin(\cos^{-1} t')} \sin\phi \, \hat{\theta}' + \left[\frac{H_{s\theta}(\phi \to \cos^{-1} t')}{\sin(\cos^{-1} t')} (\cos\phi \cos\theta' + t' \sin\theta' \cot\theta_o) \right. \right.$$

$$\left. \left. + H_{s\phi}(\phi \to \cos^{-1} t') \frac{\sin\theta'}{\sin\theta_o} \right] \hat{\phi} \right\}, \; t' = \frac{\sin\theta' \cos\phi}{\sin\theta_o}. \tag{31}$$

Since ϕ', the azimuth coordinate of the field point relative to the point of integration, is a constant for all z', we have set ϕ' equal to ϕ in (31).

For large $k\rho$, the integral (28) is asymptotically approximated by the stationary phase formula[29]

$$\int_{-\infty}^{\infty} e^{ik\rho q(z')} \hat{f}(z') dz' \underset{\rho \to \infty}{\sim} e^{ik\rho q(z'_s) + i\mu\pi/4} \left(\frac{2\pi}{k\rho |q''(z'_s)|} \right)^{1/2} \hat{f}(z'_s) \tag{32}$$

where z'_s is the point of stationary phase defined by

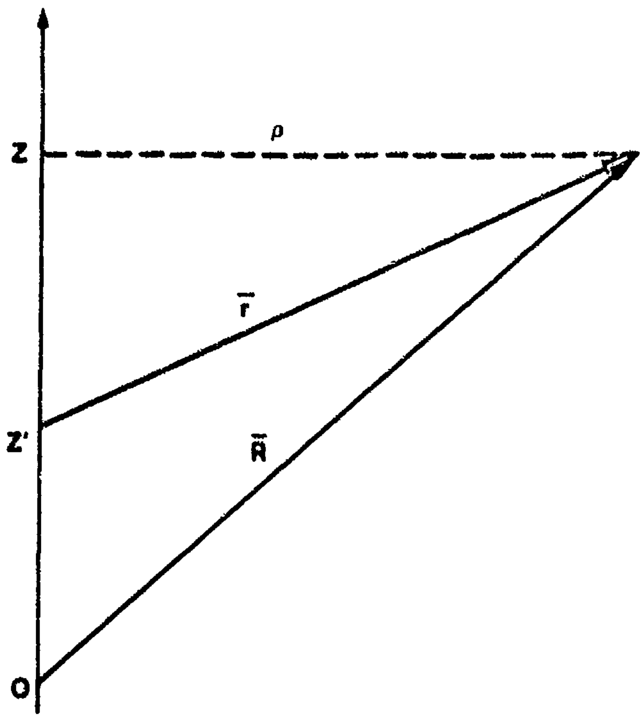

Figure 2. Geometry of Integration of the Incremental Far Field

$$q'(z'_s) = 0$$

and

$$\mu = \text{sign } q''(z'_s).$$

Differentiating (30),

$$q'(z') = \frac{1}{\rho}\left(\frac{dr}{dz'} - \cos\theta_o\right) \tag{33}$$

and since

$$r = [\rho^2 + (z' - z)^2]^{1/2}, \tag{34}$$

$$\frac{dr}{dz'} = \frac{z' - z}{r} = -\cos\theta'. \tag{35}$$

Equating (33) to zero then gives $\cos\theta'$ at $z = z'_s$,

$$\cos\theta'_s = -\cos\theta_o. \tag{36}$$

It follows easily, using (34) and (35), that

$$r_s = \frac{\rho}{\sin\theta_o} \tag{37}$$

so that

$$z'_s = \rho\,(\cot\theta_o + \cot\theta)$$

and hence

$$q'(z'_s) = \frac{1}{\sin\theta_o} - \cos\theta_o\,(\cot\theta_o + \cot\theta). \tag{38}$$

Moreover, differentiating (33), using (35), and substituting (36) and (37) yields

$$q''(z_s') = \frac{\sin^3\theta_o}{\rho^2} \tag{39}$$

which implies that μ in (32) is positive. Also, since

$$\sin\theta' = \frac{\rho}{r},$$

$$\sin\theta_s' = \frac{\rho}{r_s} = \sin\theta_o \tag{40}$$

from which

$$t_s' = \cos\phi \tag{41}$$

and hence,

$$\sin(\cos^{-1} t_s') = \sin\phi. \tag{42}$$

Since

$$\hat{\theta}' = \hat{x}\cos\theta'\cos\phi + \hat{y}\cos\theta'\sin\phi - \hat{z}\sin\theta',$$

substitution of (36) and (40) yields

$$\hat{\theta}'_s = \hat{\theta}_o^{\pi} \equiv \hat{\theta}\,\big|_{\theta=\pi-\theta_o}. \tag{43}$$

Finally, substituting (38), (39), (36), (40), (41), (42), and (43) in (32), and using the readily obtained expression for $\hat{r}_o\cdot\bar{R}$,

$$\hat{r}_o\cdot\bar{R} = -\frac{\rho}{\sin\theta}\cos(\theta + \theta_o)$$

yields the desired relation

$$\int_{-\infty}^{\infty} d\overline{H}_s(\overline{r}) \underset{\rho \to \infty}{\sim} H_{s\theta}\, \hat{\theta}_o^{\pi} + H_{s\phi}\, \hat{\phi}. \tag{44}$$

4.2 Comparison With Michaeli's Incremental Diffraction Coefficients for the Perfectly Conducting Half-Plane and Infinite Wedge

As a second check on the expressions we have derived for the incremental far fields of planar surfaces, we obtain the incremental far fields for the particular cases of a half plane and infinite wedge, and show that these fields agree with the expressions obtained independently by Michaeli[18] from integration of the surface currents.

4.2.1 HALF-PLANE ILLUMINATED BY A PLANE WAVE

We specialize (24a, b) to the case of a half-plane illuminated by a plane wave. The half-plane is defined in terms of Cartesian coordinates (x, y, z) by the equation $y = 0$, $x \geq 0$, so that the edge of the half-plane coincides with the z-axis. The direction vector of the incident plane wave forms angles of $\pi + \phi_0$ and $\pi - \theta_0$ with the positive x-axis and z-axis respectively (see Figure 3).

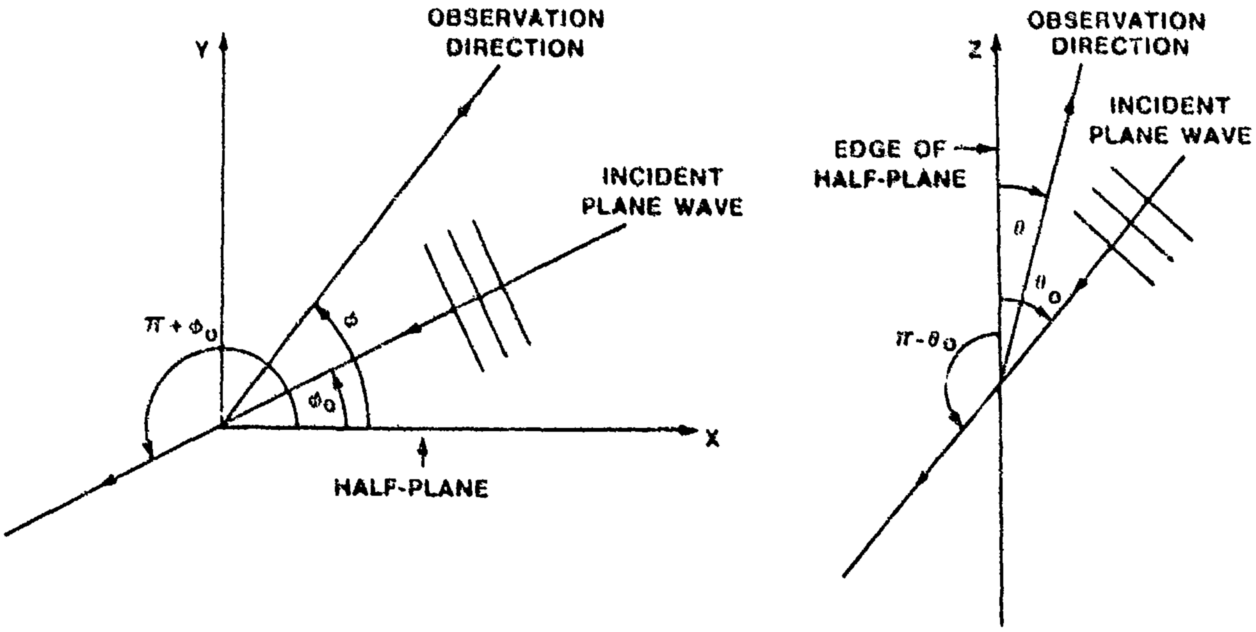

Figure 3. Geometry of a Half-Plane Illuminated by a Plane Wave

We begin with a TM (E-polarized) incident plane wave for which

$$\bar{E}_i = -E_i \exp\left[-ik\rho \sin\theta_o \cos(\phi - \phi_o) - ikz \cos\theta_o\right] \hat{\theta}_o \tag{45}$$

where E_i is the complex electric field amplitude of the plane wave. For $\theta_o = \pi/2$ (that is, the incident plane wave propagating normal to the z-axis), the scattered electric far field is given by[30]

$$E_{sz} \underset{\rho\to\infty}{\sim} E_i\left(\frac{2}{\pi k\rho}\right)^{1/2} e^{i(k\rho + \pi/4)} \frac{\sin\frac{\phi}{2}\sin\frac{\phi_o}{2}}{\cos\phi + \cos\phi_o}, \quad 0 < \phi < 2\pi,$$

from which it can be shown[25,31] that the scattered electric far field corresponding to oblique incidence is

$$\bar{E}_s \underset{\rho\to\infty}{\sim} -E_i\left(\frac{2}{\pi k\rho \sin\theta_o}\right)^{1/2} e^{i(k\rho \sin\theta_o + \pi/4)} e^{-ikz\cos\theta_o} \cdot \frac{\sin\frac{\phi}{2}\sin\frac{\phi_o}{2}}{\cos\phi + \cos\phi_o} \hat{\theta}_o^{\pi} \tag{46}$$

$$\equiv E_{s\theta}\hat{\theta}_o^{\pi}.$$

Substituting (46) in (24b), noting that $\hat{r}_o \cdot \bar{r}$ in the exponential factor of C_o is equal to $\rho \sin\theta_o - z\cos\theta_o$, and replacing the magnitude, E_i, of the incident plane wave by $E_{iz}/\sin\theta_o$, we obtain

$$\overline{dE}_s^{TM}(\bar{r}) \underset{r\to\infty}{\sim} -dz' E_{iz} \frac{\sin\theta}{\sin^2\theta_o} \frac{e^{ikr}}{4\pi r} \frac{4\sin\frac{\alpha}{2}\sin\frac{\phi_o}{2}}{\cos\alpha + \cos\phi_o} \hat{\theta}, \tag{47}$$

$$\alpha = \cos^{-1}\left(\frac{\sin\theta\cos\phi}{\sin\theta_o}\right).$$

To compare (47) with Michaeli's expression, we start with Michaeli's Eq. (1),[18] which, after specializing to an edge discontinuity coinciding with the z-axis and noting the correspondences $j \to -i$, $\hat{s} \leftrightarrow \hat{r}$, $\hat{t} \leftrightarrow \hat{z}$ between his notation and ours, yields

$$\overline{dE} \underset{r\to\infty}{\sim} -ik \frac{e^{ikr}}{4\pi r} \sin\theta[Z_o I(z')\hat{\theta} - M(z')\hat{\phi}]dz' \tag{48}$$

where I and M are the electric and magnetic equivalent currents, respectively. Expressions for I and M for a wedge with exterior angle $N\pi$ are given in Michaeli's Eq. (31). For TM incident illumination $M = 0$, and Michaeli's Eq. (31) with $N = 2$ gives

$$I = E_{iz}\frac{i}{kZ_o}\frac{\sin\frac{\phi_o}{2}}{\sin^2\theta_o}\left(\frac{1}{\cos\frac{\pi-\alpha}{2}-\cos\frac{\phi_o}{2}}+\frac{1}{\cos\frac{\pi-\alpha}{2}+\cos\frac{\phi_o}{2}}\right)$$

$$= -E_{iz}\frac{i}{kZ_o}\frac{1}{\sin^2\theta_o}\frac{4\sin\frac{\alpha}{2}\sin\frac{\phi_o}{2}}{\cos\alpha+\cos\phi_o}, \tag{49}$$

$$\alpha = \cos^{-1}\left(\frac{\sin\theta\cos\phi}{\sin\theta_o}\right),$$

where we have used the correspondences $\beta' \leftrightarrow \pi - \theta_o$, $\beta \leftrightarrow \theta$, and $\phi' \leftrightarrow \phi_o$ between Michaeli's notation and ours. Substituting (49) in (48), with $M = 0$, is then seen to give an expression for the incremental far field identical with (47).

Next, we consider a half-plane illuminated by a TE (H-polarized) incident plane wave for which

$$\overline{H}_i = -H_i \exp\left[-ik\rho\sin\theta_o\cos(\phi-\phi_o) - ikz\cos\theta_o\right]\hat{\theta}_o \tag{50}$$

where H_i is the complex magnetic field amplitude of the plane wave. For $\theta_o = \pi/2$, the scattered magnetic far field is given by[30]

$$H_{sz} \underset{\rho\to\infty}{\sim} -H_i\left(\frac{2}{\pi k\rho}\right)^{1/2} e^{i(k\rho+\pi/4)}\frac{\cos\frac{\phi}{2}\cos\frac{\phi_o}{2}}{\cos\phi+\cos\phi_o},\ 0 < \phi < 2\pi,$$

from which the scattered magnetic far field corresponding to oblique incidence is[25,31]

$$\overline{H}_s \underset{\rho\to\infty}{\sim} H_i\left(\frac{2}{\pi k\rho\sin\theta_o}\right)^{1/2} e^{i(k\rho\sin\theta_o+\pi/4)}\, e^{-ikz\cos\theta_o}\frac{\cos\frac{\phi}{2}\cos\frac{\phi_o}{2}}{\cos\phi+\cos\phi_o}\,\hat{\theta}_o^{\pi} \tag{51}$$

$$\equiv H_{s\theta}\,\hat{\theta}_o^{\pi}.$$

Substituting (51) in (24a) using [cf. (13b)] $E_{s\theta} = -Z_o H_{s\phi}$, simplifying algebraically, and replacing H_i by $H_{iz}/\sin\theta_o$, one finds

$$\overline{dE}_s^{TE}(\bar{r}) \underset{r\to\infty}{\sim} -dz'\, Z_o\frac{H_{iz}}{\sin\theta_o}\frac{e^{ikr}}{4\pi r}\frac{4\cos\frac{\alpha}{2}\cos\frac{\phi_o}{2}}{\cos\alpha+\cos\phi_o}\frac{1}{\sin\alpha}$$

$$\cdot\left[\sin\phi\,\hat{\phi} - (\cos\phi\cos\theta + \cos\alpha\sin\theta\cot\theta_o)\hat{\theta}\right], \tag{52}$$

$$\alpha = \cos^{-1}\left(\frac{\sin\theta\cos\phi}{\sin\theta_o}\right)$$

Michaeli's expression is again given by (48) with I and M defined by his Eq. (31) with N = 2. We obtain

$$I = \frac{iH_{iz}}{k\sin\theta_o}\left[\frac{\sin\theta\cos\phi}{\sin\theta_o}\left(\frac{-\cos\theta_o}{\sin\theta_o}\right) - \frac{\cos\theta}{\sin\theta}\cos\phi\right]$$

$$\cdot \sin\frac{\pi-\alpha}{2}\left(\frac{1}{\cos\frac{\pi-\alpha}{2} - \cos\frac{\phi_o}{2}} - \frac{1}{\cos\frac{\pi-\alpha}{2} + \cos\frac{\phi_o}{2}}\right)$$

$$= \frac{iH_{iz}}{k\sin\theta_o}\,\frac{4\cos\frac{\alpha}{2}\cos\frac{\phi_o}{2}}{\cos\alpha + \cos\phi_o}\,\frac{1}{\sin\alpha\sin\theta}\,(\cos\phi\cos\theta + \cos\alpha\sin\theta\cot\theta_o) \tag{53}$$

and

$$M = \frac{-iH_{iz}Z_o}{k\sin\theta\sin\theta_o}\,\frac{\sin\phi\sin\frac{\pi-\alpha}{2}}{\sin\alpha}\left(\frac{1}{\cos\frac{\pi-\alpha}{2} - \cos\frac{\phi_o}{2}} - \frac{1}{\cos\frac{\pi-\alpha}{2} + \cos\frac{\phi_o}{2}}\right)$$

$$= \frac{iZ_oH_{iz}}{k\sin\theta\sin\theta_o}\,\frac{\sin\phi\cos\frac{\alpha}{2}}{\sin\alpha}\,\frac{4\cos\frac{\phi_o}{2}}{\cos\alpha + \cos\phi_o}. \tag{54}$$

Substituting (53) and (54) in (48) yields an expression for the incremental far field identical with (52).

4.2.2 INFINITE WEDGE ILLUMINATED BY A PLANE WAVE

We now apply (24a, b) to an infinite wedge illuminated by a plane wave. The wedge is defined in terms of either a circular cylindrical coordinate system (ρ, ϕ, z) or a spherical coordinate system (r, θ, ϕ) by the equations $\phi = 0$ (face 1) and $\phi = N\pi$ (face 2), $0 \le N \le 2$, with the edge coincident with the z-axis. The direction vector of the illuminating plane wave forms angles of $\pi + \phi_o$ and $\pi - \theta_o$ with the positive x-axis and z-axis, respectively (see Figure 4).

As with the half-plane, we begin with a TM incident plane wave with the incident electric field given by (45). To apply (24b), we require expressions for the far-zone electric field radiated separately by the current on each of the faces of the wedge. Michaeli[32] has derived expressions for the contributions, E_{1sz} and E_{2sz}, of each of the wedge faces to the total diffracted field when the incident wave vector is normal to the edge of the wedge ($\theta_o = \pi/2$). For a TM incident wave

$$E_{1sz} = E_i\,[f(-\Phi_1^i) - f(-\Phi_1^r)] \tag{55}$$

$$E_{2sz} = E_i\,[f(-\Phi_2^i) - f(\Phi_2^r)] \tag{56}$$

where

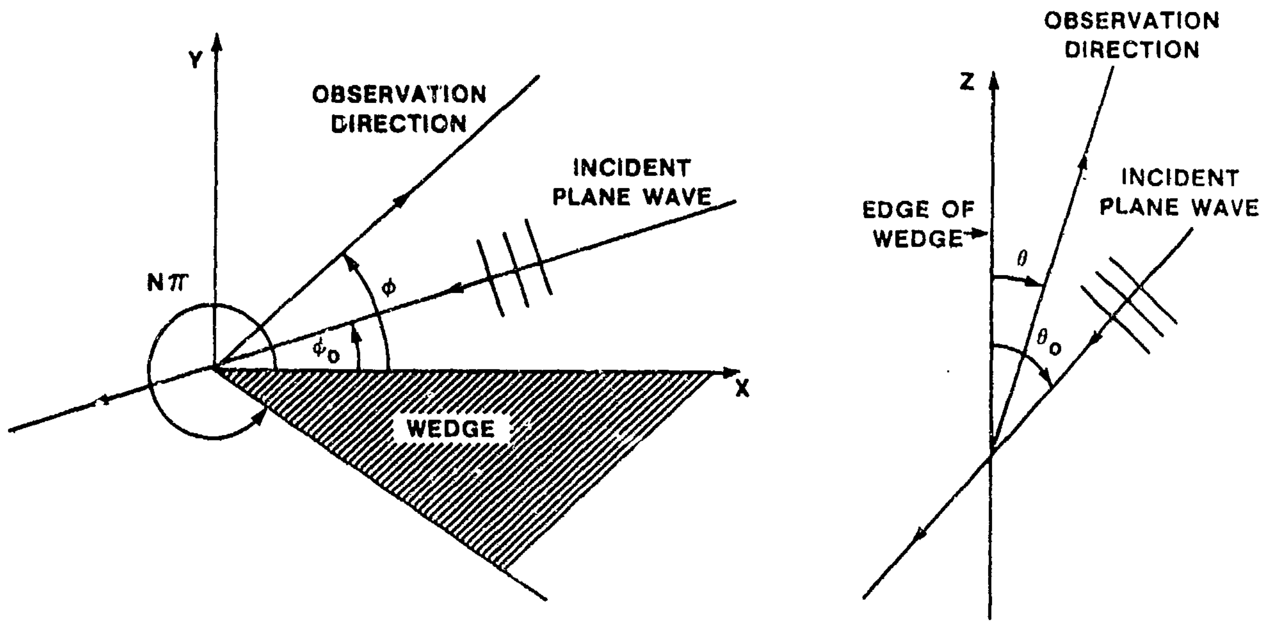

Figure 4. Geometry of a Wedge Illuminated by a Plane Wave

$$\Phi_1^i = \phi - \phi_o, \; \Phi_1^r = \phi + \phi_o$$

$$\Phi_2^{i,r} = \Phi_1^{i,r} \Big|_{\substack{\phi \to N\pi - \phi \\ \phi_o \to N\pi - \phi_o}}$$

and

$$f(\Phi) = \frac{1}{4\pi N} \int_{\pi - i\infty}^{\pi + i\infty} \cot\left(\frac{\nu + \Phi}{2N}\right) e^{-ik\rho \cos\nu} \, d\nu. \qquad (57)$$

Making the substitution $\nu = \pi + i\zeta$ in (57) and evaluating the resulting integral by the method of stationary phase yields

$$f(\Phi) \underset{\rho \to \infty}{\sim} -\frac{1}{4\pi N} \cot\left(\frac{\pi + \Phi}{2N}\right) \left(\frac{2\pi}{k\rho}\right)^{1/2} e^{i(k\rho + \pi/4)} \qquad (58)$$

from which, with the aid of some elementary trigonometric identities, (55) and (56) yield

$$E_{1sz} \underset{\rho\to\infty}{\sim} E_i\left(\frac{2}{\pi k\rho}\right)^{1/2} e^{i(k\rho + \pi/4)} \frac{\sin\frac{\phi_o}{N}}{2N\left(\cos\frac{\phi_o}{N} - \cos\frac{\pi - \phi}{N}\right)}, \; 0 < \phi < 2\pi,$$

and

$$E_{2sz} \underset{\rho\to\infty}{\sim} E_i\left(\frac{2}{\pi k\rho}\right)^{1/2} e^{i(k\rho + \pi/4)} \frac{\sin\frac{\phi_o}{N}}{2N\left(\cos\frac{\phi_o}{N} - \cos\frac{\pi + \phi}{N}\right)}, \; -(2 - N)\pi < \phi < N\pi.$$

Just as for the half-plane diffraction discussed in Section 4.2.1, the scattered electric far fields corresponding to oblique incidence of the illuminating plane wave are then

$$\bar{E}_{1s} \underset{\rho\to\infty}{\sim} - E_i\left(\frac{2}{\pi k\rho \sin\theta_o}\right)^{1/2} e^{i(k\rho \sin\theta_o + \pi/4)} e^{-ikz\cos\theta_o} \cdot \frac{\sin\frac{\phi_o}{N}}{2N\left(\cos\frac{\phi_o}{N} - \cos\frac{\pi - \phi}{N}\right)} \hat{\theta}_o^{\pi}, \; 0 < \phi < 2\pi,$$
$$\equiv E_{1s\theta}\, \hat{\theta}_o^{\pi} \tag{59}$$

and

$$\bar{E}_{2s} \underset{\rho\to\infty}{\sim} E_i\left(\frac{2}{\pi k\rho \sin\theta_o}\right)^{1/2} e^{i(k\rho \sin\theta_o + \pi/4)} e^{-ikz\cos\theta_o} \cdot \frac{\sin\frac{\phi_o}{N}}{2N\left(\cos\frac{\phi_o}{N} - \cos\frac{\pi + \phi}{N}\right)} \hat{\theta}_o^{\pi}, \; -(2 - N)\pi < \phi < N\pi,$$
$$\equiv E_{2s\theta}\, \hat{\theta}_o^{\pi}. \tag{60}$$

Now, while $E_{1s\theta}$ can be used directly in (24b) to calculate the contribution of the upper face of the wedge to the incremental electric far field, $E_{2s\theta}$ cannot, since the current sheet is not in the xz-plane as was assumed in the derivation of (24). Hence, we first transform to a (ρ, ϕ', z) coordinate system with

$$\phi' = \phi + (2 - N)\pi, \quad \phi = \phi' - (2 - N)\pi \tag{61}$$

so that $\phi' = 0$ is the equation of face 2 of the wedge. Substituting (61) in (60) gives

$$\bar{E}_{2s} \underset{\rho\to\infty}{\sim} E_i\left(\frac{2}{\pi k\rho \sin\theta_o}\right)^{1/2} e^{i(k\rho \sin\theta_o + \pi/4)}\, e^{-ikz\cos\theta_o} \tag{62}$$

$$\cdot \frac{\sin\frac{\phi_o}{N}}{2N\left(\cos\frac{\phi_o}{N} + \cos\frac{\pi - \phi'}{N}\right)}$$

$$\equiv E_{2s\theta}\, \hat{\theta}_o^{\pi}.$$

Substituting (59) and (62) in (24b) then yields

$$\overline{dE}_s^{TM}(\bar{r}) = \overline{dE}_{1s}^{TM}(\bar{r}) + \overline{dE}_{2s}^{TM}(\bar{r}) \tag{63}$$

with

$$\overline{dE}_{1s}^{TM}(\bar{r}) \underset{r\to\infty}{\sim} -dz'\, E_{iz}\frac{\sin\theta}{\sin^2\theta_o}\, \frac{e^{ikr}}{4\pi r}\, \frac{2\sin\frac{\phi_o}{N}}{N\left(\cos\frac{\phi_o}{N} - \cos\frac{\pi - \alpha_1}{N}\right)}\, \hat{\theta}, \tag{64}$$

$$\alpha_1 = \cos^{-1}\left(\frac{\sin\theta \cos\phi}{\sin\theta_o}\right),\ 0 < \phi < 2\pi,$$

and

$$\overline{dE}_{2s}^{TM}(\bar{r}) \underset{r\to\infty}{\sim} -dz'\, E_{iz}\frac{\sin\theta}{\sin^2\theta_o}\, \frac{e^{ikr}}{4\pi r}\, \frac{2\sin\frac{\phi_o}{N}}{N\left(\cos\frac{\phi_o}{N} + \cos\frac{\pi - \alpha_2}{N}\right)}\, \hat{\theta}, \tag{65}$$

$$\alpha_2 = \cos^{-1}\left(\frac{\sin\theta \cos\phi'}{\sin\theta_o}\right) \overset{(61)}{=} \cos^{-1}\left[\frac{\sin\theta\cos(N\pi - \phi)}{\sin\theta_o}\right],$$

$$-(2 - N)\pi < \phi < N\pi.$$

Michaeli's expression[18] for the incremental far field is given by (48) with $M = 0$ (TM illumination) and

$$I = E_{iz}\frac{2i}{kZ_o}\, \frac{\sin\frac{\phi_o}{N}}{\sin^2\theta_o}\left(\frac{1}{\cos\frac{\pi - \alpha_1}{N} - \cos\frac{\phi_o}{N}} + \frac{1}{\cos\frac{\pi - \alpha_2}{N} + \cos\frac{\phi_o}{N}}\right)$$

which is seen to be identical to our expression given by (63) with (64) and (65).

Next, we turn to the incremental diffraction coefficient for an infinite wedge illuminated by the TE (H-polarized) incident field given by (50). Michaeli's expressions[32] for the contributions, H_{1sz} and H_{2sz}, of face 1 and face 2, respectively, to the total diffracted magnetic field when the incident wave vector is normal to the edge of the wedge are

$$H_{1sz} = H_i\,[f(-\Phi_1^i) + f(-\Phi_1^r)]$$

$$H_{2sz} = H_i\,[f(\Phi_2^i) + f(\Phi_2^r)]$$

with $f(\Phi)$ given in general by (57) and for large $k\rho$ by (58), and $\Phi_{1,2}$ defined as for TM incidence. Similar to the TM case, we find that

$$H_{1sz} \underset{\rho\to\infty}{\sim} - H_i\left(\frac{2}{\pi k\rho}\right)^{1/2} e^{i(k\rho + \pi/4)} \frac{\sin\frac{\pi - \phi}{N}}{2N\left(\cos\frac{\phi_o}{N} - \cos\frac{\pi - \phi}{N}\right)},\ 0 < \phi < 2\pi,$$

and

$$H_{2sz} \underset{\rho\to\infty}{\sim} - H_i\left(\frac{2}{\pi k\rho}\right)^{1/2} e^{i(k\rho + \pi/4)} \frac{\sin\frac{\pi + \phi}{N}}{2N\left(\cos\frac{\phi_o}{N} - \cos\frac{\pi + \phi}{N}\right)},\ -(2 - N)\pi < \phi < N\pi.$$

Then, like the half-plane diffraction discussed in Section 4.2.1, the scattered magnetic far fields corresponding to oblique incidence of the illuminating plane wave are

$$\bar{H}_{1s} \underset{\rho\to\infty}{\sim} H_i\left(\frac{2}{\pi k\rho \sin\theta_o}\right)^{1/2} e^{i(k\rho\sin\theta_o + \pi/4)}\, e^{-ikz\cos\theta_o} \cdot \frac{\sin\frac{\pi - \phi}{N}}{2N\left(\cos\frac{\phi_o}{N} - \cos\frac{\pi - \phi}{N}\right)}\,\hat{\theta}_o^{\pi},\ 0 < \phi < 2\pi, \tag{66}$$

$$\equiv H_{1s\theta}\,\hat{\theta}_o^{\pi},$$

and

$$\bar{H}_{2s} \underset{\rho\to\infty}{\sim} H_i\left(\frac{2}{\pi k\rho \sin\theta_o}\right)^{1/2} e^{i(k\rho\sin\theta_o + \pi/4)}\, e^{-ikz\cos\theta_o} \cdot \frac{\sin\frac{\pi + \phi}{N}}{2N\left(\cos\frac{\phi_o}{N} - \cos\frac{\pi + \phi}{N}\right)}\,\hat{\theta}_o^{\pi},\ -(2 - N)\pi < \phi < N\pi, \tag{67}$$

$$\equiv H_{2s\theta}\,\hat{\theta}_o^{\pi}.$$

As done above in treating the TM case, we transform (67) to the (ρ, ϕ', z) coordinate system with ϕ' defined by (61), obtaining

$$\overline{H}_{2s} \underset{\rho\to\infty}{\sim} H_i \left(\frac{2}{\pi k\rho \sin\theta_o}\right)^{1/2} e^{i(k\rho\sin\theta_o + \pi/4)}\, e^{-ikz\cos\theta_o} \tag{68}$$

$$\cdot \frac{\sin\frac{\pi-\phi'}{N}}{2N\left(\cos\frac{\phi_o}{N} + \cos\frac{\pi-\phi'}{N}\right)}\, \hat{\theta}_o^{\pi},$$

$$\equiv H_{2s\theta}\, \hat{\theta}_o^{\pi}.$$

Use of [cf. (13b)] $E_{s\phi} = -Z_o H_{s\theta}$, and substitution of (66) and (68) into (24a) then yields

$$\overline{dE}_s^{TE}(\bar{r}) = \overline{dE}_{1s}^{TE}(\bar{r}) + \overline{dE}_{2s}^{TE}(\bar{r}) \tag{69}$$

with

$$\overline{dE}_{1s}^{TE}(\bar{r}) \underset{r\to\infty}{\sim} -dz'\, Z_o \frac{H_{iz}}{\sin\theta_o} \frac{e^{ikr}}{4\pi r} \frac{2\sin\frac{\pi-\alpha_1}{N}}{N\left(\cos\frac{\phi_o}{N} - \cos\frac{\pi-\alpha_1}{N}\right)} \tag{70}$$

$$\cdot \frac{1}{\sin\alpha_1}\,[\sin\phi\,\hat{\phi} - (\cos\phi\cos\theta + \cos\alpha_1 \sin\theta\cot\theta_o)\hat{\theta}],$$

$$\alpha_1 = \cos^{-1}\left(\frac{\sin\theta\cos\phi}{\sin\theta_o}\right),\; 0 < \phi < 2\pi,$$

and

$$\overline{dE}_{2s}^{TE}(\bar{r}) \underset{r\to\infty}{\sim} -dz'\, Z_o \frac{H_{iz}}{\sin\theta_o} \frac{e^{ikr}}{4\pi r} \frac{2\sin\frac{\pi-\alpha_2}{N}}{N\left(\cos\frac{\phi_o}{N} + \cos\frac{\pi-\alpha_2}{N}\right)} \tag{71}$$

$$\cdot \frac{1}{\sin\alpha_2}\,[\sin\phi'\,\hat{\phi} - (\cos\phi'\cos\theta + \cos\alpha_2 \sin\theta\cot\theta_o)\hat{\theta}],$$

$$\alpha_2 = \cos^{-1}\left(\frac{\sin\theta\cos\phi'}{\sin\theta_o}\right),\; 0 < \phi' < 2\pi,$$

Finally, we transform (71) back to the (ρ, ϕ, z) coordinate system to obtain

$$\overline{dE}^{TE}_{2s}(\bar{r}) \underset{r\to\infty}{\sim} dz' Z_o \frac{H_{iz}}{\sin\theta_o} \frac{e^{ikr}}{4\pi r} \frac{2 \sin \frac{\pi - \alpha_2}{N}}{N\left(\cos\frac{\phi_o}{N} + \cos \frac{\pi - \alpha_2}{N}\right)} \tag{72}$$

$$\cdot \frac{1}{\sin \alpha_2} [\sin (N\pi - \phi)\hat{\phi} + (\cos(N\pi - \phi)\cos\theta + \cos\alpha_2 \sin\theta \cot\theta_o)\hat{\theta}],$$

$$\alpha_2 = \cos^{-1}\left[\frac{\sin\theta \cos(N\pi - \phi)}{\sin\theta_o}\right], \; -(2 - N)\pi < \phi < N\pi.$$

Michaeli's expression [18] for the incremental far field is given by (48) with, from his Eq. (31),

$$I = \frac{iH_{iz}}{k \sin\theta_o} \frac{2}{N} \left[\frac{\frac{\sin\theta \cos\phi}{\sin\theta_o}\left(-\frac{\cos\theta_o}{\sin\theta_o}\right) - \frac{\cos\theta \cos\phi}{\sin\theta}}{\sin\alpha_1} \frac{\sin\frac{\pi - \alpha_1}{N}}{\cos\frac{\pi - \alpha_1}{N} - \cos\frac{\phi_o}{N}} \right.$$

$$\left. - \frac{\frac{\sin\theta \cos (N\pi - \phi)}{\sin\theta_o}\left(-\frac{\cos\theta_o}{\sin\theta_o}\right) - \frac{\cos\theta}{\sin\theta} \cos (N\pi - \phi)}{\sin\alpha_2} \frac{\sin\frac{\pi - \alpha_2}{N}}{\cos\frac{\pi - \alpha_2}{N} + \cos\frac{\phi_o}{N}} \right]$$

$$= \frac{-iH_{iz}}{k \sin\theta_o} \frac{2}{N\sin\theta} \left(\frac{\sin\frac{\pi - \alpha_1}{N}}{\cos\frac{\pi - \alpha_1}{N} - \cos\frac{\phi_o}{N}} \frac{\cos\phi \cos\theta + \cos\alpha_1 \sin\theta \cot\theta_o}{\sin\alpha_1} \right.$$

$$\left. - \frac{\sin\frac{\pi - \alpha_2}{N}}{\cos\frac{\pi - \alpha_2}{N} + \cos\frac{\phi_o}{N}} \frac{\cos(N\pi - \phi)\cos\theta + \cos\alpha_2 \sin\theta \cot\theta_o}{\sin\alpha_2} \right)$$

and

$$M = \frac{-iH_{iz}Z_o}{k \sin\theta \sin\theta_o} \frac{2}{N} \left[\frac{\sin\phi}{\sin\alpha_1} \frac{\sin\frac{\pi - \alpha_1}{N}}{\cos\frac{\pi - \alpha_1}{N} - \cos\frac{\phi_o}{N}} + \frac{\sin(N\pi - \phi)}{\sin\alpha_2} \frac{\sin\frac{\pi - \alpha_2}{N}}{\cos\frac{\pi - \alpha_2}{N} + \cos\frac{\phi_o}{N}} \right],$$

$$\alpha_1 = \cos^{-1}\left(\frac{\sin\theta \cos\phi}{\sin\theta_o}\right), \quad \alpha_2 = \cos^{-1}\left[\frac{\sin\theta \cos(N\pi - \phi)}{\sin\theta_o}\right].$$

His expression is thus identical with ours given by (69) with (70) and (72).

4.3 Comparison of the Physical Optics Incremental Far Fields for a Wedge With Knott's Expressions

Just as total incremental far fields are obtained by our method starting with the total cylindrical far field, one can obtain physical optics incremental far fields by starting with expressions for the cylindrical PO far field. Such PO incremental far fields are important since, in practical computational applications, it is often desired to supplement the PO far field (obtained by numerical integration of the PO surface currents) with the far field radiated by the nonuniform currents. This latter far field can then be obtained by integrating the nonuniform current incremental far field that has been found by subtracting the PO incremental far field from the total incremental far field.

In this section, we derive PO incremental far fields for the wedge and compare these with expressions given by Knott,[19,33] who shows that the difference between Michaeli's[18] and Mitzner's[17] incremental far fields are simply the PO incremental far fields. The starting point for obtaining the PO incremental far fields for the wedge is the cylindrical PO far field of each face of the wedge (see Figure 4 for the wedge geometry). In Section 4.2, to obtain expressions for the incremental total far field, we began with the two-dimensional far field corresponding to normal incidence of the illuminating plane wave, from which the cylindrical far field for oblique incidence was obtained by a simple substitution using a method described by Senior and Uslenghi[25] and Jull.[31] The same procedure cannot, in general, be used to derive the cylindrical PO far field for oblique incidence from the two-dimensional PO far field for normal incidence since, unlike the total field, the PO fields do not satisfy the boundary condition that the tangential electric field vanishes on the surfaces of the scatterer. In particular, the PO fields associated with a TE incident plane wave do not remain transverse for oblique incidence. Hence, we will obtain the cylindrical PO far field for oblique incidence directly.

We begin with a TM (E-polarized) incident plane wave with the incident electric field given by (45). The incident magnetic field is then

$$\overline{H}_i = \frac{E_i}{Z_o} \exp[-ik\rho \sin\theta_o \cos(\phi - \phi_o) - ikz \cos\theta_o]\hat{\phi}_o.$$

On face 1 of the wedge, $\phi = 0$ and the unit normal is $\hat{y}$, so that the PO current is given by

$$\overline{K}_1 = 2U_1\frac{E_i}{Z_o} \sin\phi_o \exp(-ik\rho \sin\theta_o \cos\phi_o - ikz \cos\theta_o)\hat{z} \tag{73}$$

where

$$U_1 \equiv U(\pi - \phi_o)$$

with $U(x)$ the unit step function (0 for $x < 0$, 1 for $x > 0$). On face 2 of the wedge, $\phi = N\pi$ and the unit normal is $\sin N\pi\hat{x} - \cos N\pi\hat{y}$, so that the PO current is

$$\overline{K}_2 = 2U_2\frac{E_i}{Z_o} \sin(N\pi - \phi_o) \exp[-ik\rho \sin\theta_o \cos(N\pi - \phi_o) - ikz \cos\theta_o]\hat{z} \tag{74}$$

where

$$U_2 \equiv U[\phi_o - (N - 1)\pi].$$

The PO magnetic far field may be found from (6). Since

$$\hat{r}_o \times \hat{z} = -\sin\theta_o\,\hat{\phi},$$

(6) with (73) gives

$$\overline{H}_1^{PO}(\bar{r}) \underset{r\to\infty}{\sim} -2U_1\frac{E_i}{Z_o}\,\frac{\exp[i(k\rho\sin\theta_o - kz\cos\theta_o + \frac{\pi}{4})]}{(8\pi k\rho\sin\theta_o)^{1/2}}\,\frac{\sin\phi_o}{\cos\phi_o + \cos\theta}\,\hat{\phi}$$

from which, with (13b), we obtain the PO electric far field

$$\overline{E}_1^{PO}(\bar{r}) \underset{r\to\infty}{\sim} -2U_1E_i\,\frac{\exp[i(k\rho\sin\theta_o - kz\cos\theta_o + \frac{\pi}{4})]}{(8\pi k\rho\sin\theta_o)^{1/2}}\,\frac{\sin\phi_o}{\cos\phi_o + \cos\theta}\,\hat{\theta}_o^{\pi},\ 0 < \phi < 2\pi \tag{75}$$

$$\equiv E_{1\theta}^{PO}\,\hat{\theta}_o^{\pi}.$$

For face 2 of the wedge, before applying (6), it is necessary to transform to the (ρ, ϕ' z) coordinate system with ϕ' given by (61), since (6) is based on the assumption that the current sheet is in the xz-plane. Thus, the factor $\exp(-ikx'\sin\theta_o\cos\phi)$ in (6) is replaced by

$$\exp(-ikx'\sin\theta_o\cos\phi') = \exp[-ikx'\sin\theta_o\cos(N\pi - \phi)].$$

Then (6) with (74) gives

$$\overline{H}_2^{PO}(\bar{r}) \underset{r\to\infty}{\sim} -2U_2\,\frac{E_i}{Z_o}\,\frac{\exp[i(k\rho\sin\theta_o - kz\cos\theta_o + \pi/4)]}{(8\pi k\rho\sin\theta_o)^{1/2}}\,\frac{\sin(N\pi - \phi_o)}{\cos(N\pi - \phi_o) + \cos\phi'}\,\hat{\phi}$$

and hence, using (13b),

$$\overline{E}_2^{PO}(\bar{r}) \underset{r\to\infty}{\sim} -2U_2E_i\,\frac{\exp[i(k\rho\sin\theta_o - kz\cos\theta_o + \pi/4)]}{(8\pi k\rho\sin\theta_o)^{1/2}} \tag{76}$$

$$\cdot\,\frac{\sin(N\pi - \phi_o)}{\cos(N\pi - \phi_o) + \cos\phi'}\,\hat{\theta}_o^{\pi},\ 0 < \phi' < 2\pi,$$

$$\equiv E_{2\theta}^{PO}\,\hat{\theta}_o^{\pi}$$

Substituting (75) and (76) in (17-18) or equivalently in this TM case (24b), then yields the PO incremental electric far field

$$\overline{dE}^{PO}(\bar{r}) = \overline{dE}_1^{PO}(\bar{r}) + \overline{dE}_2^{PO}(\bar{r}) \tag{77}$$

with

$$\overline{dE}_1^{PO}(\bar{r}) \underset{r\to\infty}{\sim} -dz'\, U_1 \frac{E_{iz}}{\sin\theta_o} \frac{e^{ikr}}{4\pi r} \frac{\sin\theta}{\sin\theta_o} \frac{2\sin\phi_o}{\cos\phi_o + \cos\alpha_1}\,\hat{\theta} \tag{78}$$

and

$$\overline{dE}_2^{PO}(\bar{r}) \underset{r\to\infty}{\sim} -dz'\, U_2 \frac{E_{iz}}{\sin\theta_o} \frac{e^{ikr}}{4\pi r} \frac{\sin\theta}{\sin\theta_o} \frac{2\sin(N\pi - \phi_o)}{\cos(N\pi - \phi_o) + \cos\alpha_2}\,\hat{\theta} \tag{79}$$

where

$$\alpha_1 = \cos^{-1}\left(\frac{\sin\theta \cos\phi}{\sin\theta_o}\right),\ 0 < \phi < 2\pi,$$

and

$$\alpha_2 = \cos^{-1}\left(\frac{\sin\theta \cos\phi'}{\sin\theta_o}\right) = \cos^{-1}\left[\frac{\sin\theta \cos(N\pi - \phi)}{\sin\theta_o}\right],\ -(2-N)\pi < \phi < N\pi.$$

Knott's expression [19] for the PO incremental far field is given by (48) with $M = 0$ (TM illumination) and

$$I = \frac{E_{iz} 2i\, D_{\parallel}'}{kZ_o \sin^2\theta_o}$$

with

$$D_{\parallel}' = -\left[U_1 \frac{\sin\phi_o}{\cos\phi_o + \cos\alpha_1} + U_2 \frac{\sin(N\pi - \phi_o)}{\cos(N\pi - \phi_o) + \cos\alpha_2}\right]$$

where we have made use of the correspondences $\beta \leftrightarrow \theta$, $\beta' \leftrightarrow \pi - \theta_o$, $\phi' \leftrightarrow \phi_o$, $n \leftrightarrow N$, $U^+ \leftrightarrow U_1$, $U^- \leftrightarrow U_2$, $Z \leftrightarrow Z_o$, $E_{it} \leftrightarrow E_{iz}$, and $I_e \leftrightarrow I$ between Knott's notation and ours. Knott's expression is thus seen to agree with our expression given by (77) with (78) and (79).

We now obtain the PO incremental diffraction coefficient for an infinite wedge illuminated by the TE (H-polarized) incident field given by (50). On face 1, the PO surface current is

$$\overline{K}_1 = 2U_1H_i \exp(-ik\rho \sin\theta_o \cos\phi_o - ikz \cos\theta_o)(\sin\theta_o\hat{x} + \cos\theta_o \cos\phi_o\hat{z}),$$

while, on face 2, the PO current is found to be

$$\overline{K}_2 = -2U_2H_i \exp[-ik\rho \sin\theta_o \cos(N\pi - \phi_o) - ikz \cos\theta_o]$$

$$\cdot [\cos N\pi \sin\theta_o\hat{x} + \sin N\pi \sin\theta_o\hat{y} + \cos\theta_o \cos(N\pi - \phi_o)\hat{z}].$$

We next apply (6) to find the PO magnetic far field. Since

$$\hat{r}_o \times (\sin\theta_o\hat{x} + \cos\theta_o \cos\phi_o\hat{z}) = \sin\theta_o[\sin\phi\hat{\theta}_o^{\pi} - \cos\theta_o(\cos\phi_o + \cos\phi)\hat{\phi}]$$

[recall that $(\hat{r}_o, \hat{\theta}_o^{\pi}, \hat{\phi})$ are the standard $(\hat{r}, \hat{\theta}, \hat{\phi})$ spherical coordinate system unit vectors evaluated at $\theta = \pi - \theta_o$ and ϕ]

$$\overline{H}_1^{PO}(\bar{r}) \underset{r\to\infty}{\sim} 2U_1H_i \frac{\exp[i(k\rho \sin\theta_o - kz \cos\theta_o + \pi/4)]}{(8\pi k\rho \sin\theta_o)^{1/2}} \frac{1}{\cos\phi_o + \cos\phi}$$

$$\cdot [\sin\phi\, \hat{\theta}_o^{\pi} - \cos\theta_o (\cos\phi_o + \cos\phi)\hat{\phi}]$$

$$\equiv H_{1\theta}^{PO}\, \hat{\theta}_o^{\pi} + H_{1\phi}^{PO}\, \hat{\phi},$$

from which (17) and (18) yield the PO incremental electric far field for face 1 of the wedge

$$\overline{dE}_1^{PO}(\bar{r}) \underset{r\to\infty}{\sim} -dz'\, U_1 Z_o \frac{H_{iz}}{\sin\theta_o} \frac{e^{ikr}}{4\pi r} \frac{2}{\cos\phi_o + \cos\alpha_1}$$

$$\cdot \{\sin\phi\, \hat{\phi} - (\cos\phi \cos\theta - \cos\phi_o \sin\theta \cot\theta_o)\hat{\theta}\} \tag{80}$$

$$\alpha_1 = \cos^{-1}\left(\frac{\sin\theta \cos\phi}{\sin\theta_o}\right), \; 0 < \phi < 2\pi.$$

For face 2 of the wedge,

$$\hat{r}_o \times [\cos N\pi \sin\theta_o \hat{x} + \sin N\pi \sin\theta_o \hat{y} + \cos\theta_o \cos(N\pi - \phi_o)\hat{z}]$$

$$= -\sin\theta_o \{\sin(N\pi - \phi)\hat{\theta}_o^{\pi} + \cos\theta_o[\cos(N\pi - \phi_o) + \cos(N\pi - \phi)]\hat{\phi}\}.$$

Transforming to the (ρ, ϕ', z) coordinate system with ϕ' given by (61) so that

$$\sin(N\pi - \phi) = -\sin\phi'$$

$$\cos(N\pi - \phi) = \cos\phi'$$

and applying (6), the PO magnetic far field is found to be

$$\overline{H}_2^{PO}(\hat{r}) \underset{r\to\infty}{\sim} 2U_2H_i \frac{\exp[i(k\rho \sin\theta_o - kz\cos\theta_o + \pi/4)]}{(8\pi k\rho \sin\theta_o)^{1/2}}$$

$$\cdot \frac{1}{\cos(N\pi - \phi_o) + \cos\phi'} \{-\sin\phi'\hat{\theta}_o^{\pi} + \cos\theta_o[\cos(N\pi - \phi_o) + \cos\phi']\hat{\phi}\}$$

$$\equiv H_{2\theta}^{PO}\hat{\theta}_o^{\pi} + H_{2\phi}^{PO}\hat{\phi},$$

from which, with (17) and (18), we obtain the PO incremental electric far field for face 2 of the wedge.

$$\overline{dE}_2^{PO}(\hat{r}) \underset{r\to\infty}{\sim} dz' U_2 Z_o \frac{H_{iz}}{\sin\theta_o} \frac{e^{ikr}}{4\pi r} \frac{2}{\cos(N\pi - \phi_o) + \cos\alpha_2}$$

$$\{\sin\phi'\hat{\phi} - [\cos\phi'\cos\theta - \cos(N\pi - \phi_o)\sin\theta\cot\theta_o]\hat{\theta}\}$$

$$= -dz' U_2 Z_o \frac{H_{iz}}{\sin\theta_o} \frac{e^{ikr}}{4\pi r} \frac{2}{\cos(N\pi - \phi_o) + \cos\alpha_2} \tag{81}$$

$$\cdot\{\sin(N\pi - \phi)\hat{\phi} + [\cos(N\pi - \phi)\cos\theta - \cos(N\pi - \phi_o)\sin\theta\cot\theta_o]\hat{\theta}\}$$

$$\alpha_2 = \cos^{-1}\left(\frac{\sin\theta\cos\phi'}{\sin\theta_o}\right) = \cos^{-1}\left[\frac{\sin\theta\cos(N\pi - \phi)}{\sin\theta_o}\right], \quad -(2 - N)\pi < \phi < N\pi$$

Thus, the PO incremental electric far field for the wedge for TE illumination is

$$\overline{dE_1^{PO}}\,(\bar{r}) = \overline{dE_1^{PO}}\,(r) + \overline{dE_2^{PO}}\,(\bar{r}) \tag{82}$$

with $\overline{dE_1^{PO}}$ and $\overline{dE_2^{PO}}$ given by (80) and (81), respectively.

Knott's expression[19] for the TE incremental PO electric far field for the wedge is given by (48) with

$$I = \frac{H_{iz}2iD_x'}{k\sin^2\theta_o}, \quad M = \frac{-H_{iz}2i\,Z_oD_\perp'}{k\sin\theta_o\sin\theta},$$

$$D_x' = -U_1\left(\frac{Q\cos\phi}{\cos\phi + \cos\alpha_1} + \cos\theta_o\right) + U_2\left[\frac{Q\cos(N\pi - \phi)}{\cos(N\pi - \phi_o) + \cos\alpha_2} + \cos\theta_o\right],$$

$$D_\perp' = U_1\frac{\sin\phi}{\cos\phi_o + \cos\alpha_1} - U_2\frac{\sin(N\pi - \phi)}{\cos(N\pi - \phi_o) + \cos\alpha_2},$$

and

$$Q = -\frac{1 - \cos\theta\cos\theta_o}{\sin\theta\sin\theta_o}(\cos\theta + \cos\theta_o) = -\frac{\sin\theta_o}{\sin\theta}\left(\cos\theta + \frac{\sin^2\theta\cos\theta_o}{\sin\theta_o}\right),$$

where, in addition to the correspondence already noted between Knott's notation and ours, we have used $H_{it} \leftrightarrow H_{iz}$ and $I_m \leftrightarrow M$. To facilitate comparison between Knott's expression and ours, we rewrite Knott's expression in the form

$$\overline{dE^{PO}} = (dE_{1\theta}^{PO} + dE_{2\theta}^{PO})\hat{\theta} + (dE_{1\phi}^{PO} + dE_{2\phi}^{PO})\hat{\phi} \tag{83}$$

where

$$dE_{1\theta}^{PO} = -dz'\,U_1Z_o\frac{H_{iz}}{\sin\theta_o}\frac{2e^{ikr}}{4\pi r}\left[\frac{-1}{\cos\phi_o + \cos\alpha_1}(\cos\phi\cos\theta + \cos\alpha_1\sin\theta\cot\theta_o) + \sin\theta\cot\theta_o\right] \tag{84}$$

$$dE_{2\theta}^{PO} = -dz'U_2Z_o\frac{H_{iz}}{\sin\theta_o}\frac{2e^{ikr}}{4\pi r}\left[\frac{1}{\cos(N\pi-\phi_o)+\cos\alpha_2}(\cos(N\pi - \phi)\cos\theta + \cos\alpha_2\sin\theta\cot\theta_o) - \sin\theta\cot\theta_o\right] \tag{85}$$

$$dE_{1\phi}^{PO} = dz'\,U_1Z_o\frac{H_{iz}}{\sin\theta_o}\frac{e^{ikr}}{4\pi r}\frac{2\sin\phi}{\cos\phi_o + \cos\alpha_1}, \tag{86}$$

and

$$dE^{PO}_{2\phi} = -dz' \, U_{\hat{z}} Z_o \frac{H_{iz}}{\sin\theta_o} \frac{e^{ikr}}{4\pi r} \frac{2\sin(N\pi - \phi)}{\cos(N\pi - \phi_o) + \cos\alpha_2}. \quad (87)$$

Starting with the θ-terms and comparing (84) and (85) with the θ-components of (80) and (81), respectively, we see that there is complete agreement between Knott's expression and ours, while comparing (86) and (87) with the ϕ-components of (80) and (81), respectively, it is seen that there is agreement to within the sign of (86) and complete agreement of the ϕ-components for the second face of the wedge. The difference of sign between Knott's expression and ours for the ϕ-component of the incremental TE physical optics far field for face 1 is the result of a misprint in the sign of the right-hand side of Knott's Eq. (20) for $D'_{\perp}$, which he corrects in Reference 33.

In concluding this section, we want to draw attention to the essential simplicity of our method for obtaining incremental far fields. As seen above with the examples of the half-plane and infinite wedge, all that is needed is an expression for the cylindrical far field of each of the planar surfaces comprising the scattering object. The incremental far field is then obtained by straightforward substitution of the components of the cylindrical far field in the general expressions (23) and (24) or (17) and (18). No current integrations are required.

5. INCREMENTAL FAR FIELDS FOR THE INFINITE STRIP AND SLIT

We now obtain incremental far fields, total and physical optics, for the perfectly conducting infinite strip and the complementary infinite slit. To the best of our knowledge, this is the first time that such expressions have been derived. Our expressions for the total incremental far fields are given for the low frequency approximation (that is, narrow strip and slit), but the method used to obtain them is fully applicable to any size strip or slit.

5.1 Incremental Total Far Field for the Strip

Following Asvestas and Kleinman,[34] the strip of width d is defined in terms of Cartesian coordinates (x, y, z) by $y = 0$, $|x| \le d/2$, so that the strip lies in the xz-plane with the edges of the strip parallel to the z-axis; in other words, as shown in Figure 1, but with the center of the strip at $x = 0$. The direction vector of the incident plane wave forms angles of $\pi + \phi_o$ and $\pi - \theta_o$ with the positive x-axis and z-axis respectively.

We begin with a TM incident plane wave and the incident electric field given by (45). For $\theta_o = \pi/2$, the scattered electric far field is given by[34]

$$E_{sz} \underset{\rho\to\infty}{\sim} E_i \left(\frac{2}{\pi k\rho}\right)^{1/2} e^{i(k\rho + \pi/4)} P_1(\phi, \phi_o, kd)$$

where, in the low frequency approximation

$$P_1(\phi, \phi_o, kd) = \pi \sum_{n=0}^{2} T_{2n}(\phi, \phi_o; p)\, c^{2n} + o(c^5)$$

with

$$c = \frac{1}{2} kd,$$

$$p = \ln \frac{c}{4} + \gamma - \frac{i\pi}{2},$$

$$\gamma = 0.5772157 \ldots = \text{Euler's constant},$$

$$T_o = \frac{1}{2} p,$$

$$T_2 = -\frac{1}{4} \left(\frac{\cos^2\phi}{2p} - \cos\phi_o \cos\phi - \frac{\sin^2\phi_o}{2p} \right),$$

and

$$T_4 = \frac{\cos^4\phi}{128p} - \frac{1}{32} \cos\phi_o \cos^3\phi - \frac{1}{32} \left(\frac{\sin^2\phi_o}{p} + \cos^2\phi_o - \frac{1}{2} - \frac{1}{4p} \right) \cos^2\phi$$

$$+ \frac{1}{16} \left[-\frac{1}{2} \cos^3\phi_o + \left(p + \frac{1}{4} \right) \cos\phi_o \right] \cos\phi$$

$$+ \left[\frac{\cos^4\phi_o}{128p} + \frac{1}{64} \left(1 - \frac{3}{2p} \right) \cos^2\phi_o + \frac{1}{256} \left(\frac{1}{p^2} + \frac{3}{2p} - 2 \right) \right].$$

These expressions taken from Asvestas and Kleinman[34] are valid for all values of ϕ and ϕ_o. For brevity, we have included only terms through c^4 in the series for P_1. Expressions for higher order terms are given in Asvestas and Kleinman[34] and Millar.[35] The scattered electric far field corresponding to oblique incidence is then

$$E_s \underset{\rho\to\infty}{\sim} E_i \left(\frac{2}{\pi k\rho \sin\theta_o} \right)^{1/2} e^{i(k\rho \sin\theta_o - kz \cos\theta_o + \pi/4)} P_1(\phi, \phi_o, kd \sin\theta_o) \hat{\theta}_o^{\pi} \tag{88}$$

$$\equiv E_{s\theta}\, \hat{\theta}_o^{\pi}.$$

Substitution of (88) into (24b) yields the incremental electric far field

$$\overline{dE}_s^{TM} (\bar{r}) \underset{r\to\infty}{\sim} dz' E_{iz} \frac{\sin\theta}{\sin^2\theta_o} \frac{e^{ikr}}{4\pi r} 4P_1 (\alpha, \phi_o, kd \sin\theta_o) \hat{\theta}, \tag{89}$$

$$\alpha = \cos^{-1} \left(\frac{\sin\theta \cos\phi}{\sin\theta_o} \right)$$

with the incremental magnetic far field obtained from (18)

$$\overline{dH}_s^{TM}(\bar{r}) \underset{r\to\infty}{\sim} -dz' \frac{E_{iz}}{Z_o} \frac{\sin\theta}{\sin^2\theta_o} \frac{e^{ikr}}{4\pi r} 4P_1(\alpha, \phi_o, kd \sin\phi_o)\hat{\phi}. \tag{90}$$

Next, we consider the strip illuminated by a TE (H-polarized) incident plane wave given by (50). For $\theta_o = \pi/2$, the scattered magnetic far field is given by[34]

$$H_{sz} \underset{\rho\to\infty}{\sim} H_i \left(\frac{2}{\pi k\rho}\right)^{1/2} e^{i(k\rho + \pi/4)} P_2(\phi, \phi_o, kd)$$

where, in the low frequency approximation

$$P_2(\phi, \phi_o, kd) = \pi c^2 \sum_{n=0}^{1} T_{2n}(\phi, \phi_o; p)c^{2n} + o(c^5)$$

with

$$T_o = -\frac{1}{4}\sin\phi_o \sin\phi,$$

$$T_2 = \frac{1}{16}\sin\phi_o \sin\phi\left[\frac{1}{2}\cos^2\phi + \frac{1}{2}\cos\phi_o \cos\phi + \left(p - \frac{3}{4} + \frac{1}{2}\cos^2\phi_o\right)\right],$$

and c and p are defined as for TM illumination. These expressions are valid for all values of ϕ and ϕ_o. Expressions for higher order terms in the series for P_2 are to be found in Asvestas and Kleinman[34] and Millar.[35] The scattered magnetic far field corresponding to oblique incidence of the illuminating plane wave is then

$$\bar{H}_s \underset{\rho\to\infty}{\sim} -H_i\left(\frac{2}{\pi k\rho \sin\theta_o}\right)^{1/2} e^{i(k\rho \sin\theta_o - kz\cos\theta_o + \pi/4)} P_2(\phi,\phi_o, kd \sin\theta_o)\hat{\theta}_o^{\pi} \tag{91}$$

$$\equiv H_{s\theta}\, \hat{\theta}_o^{\pi}.$$

By substituting (91) in (23a) and using (13b), we obtain the incremental magnetic far field

$$\overline{dH}_s^{TE}(\bar{r}) \underset{r\to\infty}{\sim} -dz' \frac{H_{iz}}{\sin\theta_o} \frac{e^{ikr}}{4\pi r} \frac{4P_2(\alpha, \phi, kd \sin\theta_o)}{\sin\alpha} \cdot [\sin\phi\, \hat{\theta} + (\cos\phi \cos\theta + \cos\alpha \sin\theta \cot\theta_o)\hat{\phi}] \tag{92}$$

$$\alpha = \cos^{-1}\left(\frac{\sin\theta \cos\phi}{\sin\theta_o}\right)$$

with the corresponding incremental electric far field then given by

$$\overline{dE}_s^{TE}(\bar{r}) \underset{r\to\infty}{\sim} dz'\, Z_o \frac{H_{iz}}{\sin\theta_o} \frac{e^{ikr}}{4\pi r} \frac{4P_2(\alpha, \phi_o, kd\sin\theta_o)}{\sin\alpha}$$

$$\cdot\, [\sin\phi\, \hat{\phi} - (\cos\phi\cos\theta + \cos\alpha\sin\theta\cot\theta_o)\hat{\theta}]. \tag{93}$$

5.2 Incremental Far Fields for the Infinite Slit

The slit, of width d, is defined in terms of Cartesian coordinates (x, y, z) to be complementary to the strip in the xz-plane, $y = 0$, $|x| \geq d/2$. As with the strip, the direction vector of the incident plane wave forms angles of $\pi + \phi_o$ and $\pi - \theta_o$ with the positive x-axis and z-axis, respectively. Here, we restrict ϕ_o to lie between 0 and π.

We consider first TM (E-polarization) illumination with the incident electric field given by (45). Application of Babinet's principle[36] enables us to obtain the electric far field $\bar{E}_d$ diffracted by the slit with TM illumination from the magnetic far field scattered by the strip with TE illumination.

Specifically,

$$\bar{E}_d \underset{\rho\to\infty}{\sim} -E_i \left(\frac{2}{\pi k\rho\sin\theta_o}\right)^{1/2} e^{i(k\rho\sin\theta_o - kz\cos\theta_o + \pi/4)}\, P_2(\phi, \phi_o, kd\sin\theta_o) \frac{\sin\phi}{|\sin\phi|}\, \hat{\theta}_o^{\pi} \tag{94}$$

$$\equiv E_{d\theta}\, \hat{\theta}_o^{\pi}.$$

(The total field in the illuminated half-space $y > 0$ is equal to the field that would be there if no slit were present—the incident and reflected field—plus the diffracted field, whereas, in the half-space $y < 0$ behind the screen, the total field is given by the diffracted field.) Substitution of (94) in (24b) then yields the incremental diffracted electric far field

$$\overline{dE}_d^{TM}(\bar{r}) \underset{r\to\infty}{\sim} -dz'\, E_{iz} \frac{\sin\theta}{\sin^2\theta_o} \frac{e^{ikr}}{4\pi r} 4P_2(\alpha, \phi_o, kd\sin\theta_o) \frac{\sin\phi}{|\sin\phi|}\, \hat{\theta}, \tag{95}$$

$$\alpha = \cos^{-1}\left(\frac{\sin\theta\cos\phi}{\sin\theta_o}\right),$$

with the corresponding incremental diffracted magnetic far field given by (18),

$$\overline{dH}_d^{TM}(\bar{r}) \underset{r\to\infty}{\sim} -dz' \frac{E_{iz}}{Z_o} \frac{\sin\theta}{\sin^2\theta_o} \frac{e^{ikr}}{4\pi r} 4P_2(\alpha, \phi_o, kd\sin\theta_o) \frac{\sin\phi}{|\sin\phi|}\, \hat{\phi} \tag{96}$$

Next, we treat TE (H-polarization) illumination with the incident magnetic field given by (50). Using Babinet's principle[36] again, we obtain the magnetic far field diffracted by the slit with TE illumination from the electric far field scattered by the strip with TM illumination,

$$\overline{H}_d \underset{\rho\to\infty}{\sim} -H_i \left(\frac{2}{\pi k\rho \sin\theta_o}\right)^{1/2} e^{i(k\rho\sin\theta_o - kz\cos\theta_o + \pi/4)}\, P_1(\phi, \phi_o, kd\sin\theta_o)\, \frac{\sin\phi}{|\sin\phi|}\, \hat{\theta}_o^{\pi} \tag{97}$$

$$\equiv H_{d\theta}\, \hat{\theta}_o^{\pi}$$

Substituting (97) in (23a), we obtain the incremental diffracted magnetic far field

$$\overline{dH}_d^{TE}(\bar{r}) \underset{r\to\infty}{\sim} -dz' \frac{H_{iz}}{\sin\theta_o} \frac{e^{ikr}}{4\pi r} \frac{4P_1(\alpha, \phi_o, kd\sin\theta_o)\frac{\sin\phi}{|\sin\phi|}}{\sin\alpha} \tag{98}$$

$$\cdot\, [\sin\phi\, \hat{\theta} + (\cos\phi\cos\theta + \cos\alpha\sin\theta\cot\theta_o)\hat{\phi}],\ \alpha = \cos^{-1}\left(\frac{\sin\theta\cos\phi}{\sin\theta_o}\right)$$

and the corresponding incremental diffracted electric far field is then

$$\overline{dE}_d^{TE}(\bar{r}) \underset{r\to\infty}{\sim} dz' \frac{Z_oH_{iz}}{\sin\theta_o} \frac{e^{ikr}}{4\pi r} \frac{4P_1(\alpha, \phi_o, kd\sin\theta_o)\frac{\sin\phi}{|\sin\phi|}}{\sin\alpha} \tag{99}$$

$$\cdot\, [\sin\phi\, \hat{\phi} - (\cos\phi\cos\theta + \cos\alpha\sin\theta\cot\theta_o)\hat{\theta}].$$

5.3 Incremental Physical Optics Far Field for the Strip and Slit

In obtaining incremental PO far fields for the strip and slit, it suffices to limit attention to either the strip or the slit. This is because the sum of the PO diffracted far field of the strip and complementary slit is the PO diffracted far field of the entire plane, which is equal to zero if it is assumed, as is done consistently in this report, that the PO surface current vanishes at infinity. Hence, the PO diffracted far field of the slit is the negative of the PO far field of the complementary strip.

The geometry of the strip and incident illumination are defined as in Section 5.1. We note that the PO surface currents excited on the strip for either TM or TE illumination are identical in form to those excited on face 1 of the wedge for the given illumination. Hence, in applying (6) to obtain the PO magnetic far field for the strip, the strip differs from face 1 of the wedge only in that the effective limits of the $\overline{K}(x')$ integration are -d/2 to d/2 for the strip, and zero to infinity for the wedge. Thus, the PO incremental far fields for the strip can be obtained from those found in Section 4.3 for face 1 of the wedge, (78) and (80), simply by multiplying the face 1 incremental wedge fields by the factor

$$\frac{\displaystyle\int_{-d/2}^{d/2} e^{-ikx'\sin\theta_o\cos\phi_o - ikx'\sin\theta_o\cos\phi} dx'}{\displaystyle\int_0^{\infty} e^{-ikx'\sin\theta_o\cos\phi_o - ikx'\sin\theta_o\cos\phi} dx'}$$

$$= 2i\sin\left[\frac{kd}{2}\sin\theta_o(\cos\phi_o + \cos\phi)\right]. \tag{100}$$

6. SUMMARY

After introducing incremental diffraction theory in Section 1, we derived in Sections 2 to 3.1 exact expressions (17-18) for the three-dimensional incremental diffraction coefficients in terms of the conventional, two-dimensional diffraction coefficients of perfectly conducting, planar scatterers. Section 3.2 explained how the necessary two-dimensional far-field functions are analytically continued into the domain of imaginary values of the azimuthal angle ϕ.

In Section 3.3, we showed that an isolated singularity in the two-dimensional far field transforms to a cone of singularities in the incremental far fields. Moreover, Section 3.3 showed that the exact expressions for the incremental far fields can be generalized to allow increments of current that are skewed rather than normal to the axis of the two-dimensional scatterer, merely by replacing t in (17-18) with t_ψ given in (22). When this generalization is applied to the infinite wedge and the skew angle is chosen along the grazing diffracted ray, the cone of singularities associated with the diffracted ray reduces to a single direction and the corresponding results of References 27 and 37 are obtained.

In Section 3.4, the incremental far fields were separated into TE and TM fields (23-24).

In Section 4.1, the expression (17) for the three-dimensional incremental far magnetic field was integrated over an infinite straight line to prove that the two-dimensional far magnetic field is recovered. In the remainder of Section 4, we further confirmed the validity of the general expressions by showing that PTD, GTD, and PO incremental diffraction coefficients obtained by direct substitution into (17-18) and (23-24) agree with the results of Mitzner,[27] Michaeli,[18,27] and Knott,[19,33] respectively, in the case of the infinite wedge.

In Section 5, we determined the total and PO incremental diffracted fields of the infinite strip and complementary infinite slit by direct substitution into the general expressions derived in Sections 2 to 3.

As a concluding invitation to further analysis, there remains the question of whether the method of direct substitution derived here for determining three-dimensional incremental far fields from the corresponding two-dimensional far fields can be extended, at least in some cases, to curved surfaces and penetrable scatterers.

References

1. Franceschetti, G., and Mohsen, A. (1986) Recent developments in the analysis of reflector antennas. A review, *Proc. IEE*, **133(Pt. H)**:65-76.
2. Ufimtsev, P.Ya. (1957) Approximate computation of the diffraction of plane electromagnetic waves at certain metal bodies (I and II), *Sov. Phys.-Tech. Phys.*, **27**:1708-1718. (1958) **28**:2386- 2396.
3. Ufimtsev, P.Ya. (1962) *Method of Edge Waves in the Physical Theory of Diffraction*, Sovyetskoye Radio, Moscow (available in English from NTIS, Springfield, VA 22161, AD733203).
4. Bach, H., and Viskum, H.H. (1986) Comparison of three cross-polarization prediction methods for reflector antennas, *Proc. IEE*, **133(Pt. H)**:325-326. (1987) The SNFGTD method and its accuracy, *IEEE Trans Antennas Propag.*, **AP-35**:169-175.
5. Steyskal, H., and Shore. R.A. (1984) *Simple and Efficient Computation of Reflector Antenna Aperture Distributions and Far-Field Patterns*. RADC Rept. TR-84-45, Appendix C.
6. Keller, J.B.; Keller, J.B, Lewis, R.M., and Seckler, B.D. (1957, April and May) Diffraction by an aperture (I and II), *J. Appl. Phys.*, **28**:426-444, 570-579.
7. Keller, J.B. (1962) Geometrical theory of diffraction, *J. Opt. Soc. Am.*, **52**:116-130.
8. Yaghjian, A.D., and Cote, M.G. (In press) *Bistatic Scattering From the Perfectly Conducting Cube*.
9. Van Kampen, N.G. (1949) An asymptotic treatment of diffraction problems (I and II), *Physica*. **14**:575-589. (1950) **16**:817-821.
10. Born, M., and Wolf, E. (1959-1980) *Principles of Optics* (Chap. III), Pergamon Press, Oxford, 1st through 6th eds.
11. Koujoumjian, R.G. (1975) The geometrical theory of diffraction and its application, in *Topics in Applied Physics* (Vol. 2), *Numerical and Asymptotic Techniques in Electromagnetics*, R. Mittra, Ed., Springer-Verlag, New York.
12. Schwarzschild, K. (1902) Beugung und Polarisation des Lichts durch einen Spalt, *Mathematische Annalen*, **55**:177-247. [A brief discussion in English of Schwarzschild's diffraction work is given in *The Mathematical Theory of Huygens' Principle*, Baker and Copson, 2nd ed., Section 5.1 (1950), Clarendon, Oxford.]
13. MacDonald, H.M. (1912) The effect produced by an obstacle on a train of electric waves, *Phil. Trans. Roy. Soc. London*, Series A, **212**:299-337.
14. Jones, D.S. (1964) *The Theory of Electromagnetism*, Sections 9.21, 9.22, Pergamon, New York.
15. Braunbek, W. (1950) Neue Naherungsmethode fur die Beugung am ebenen Schirm, and Zur Beugung an der Kreisscheibe, *Z. Physik*, **127**:381-390 and 405-415.
16. Yaghjian, A.D. (1984) Equivalence of surface current and aperture field integrations for reflector antennas, *IEEE Trans. Antennas Propag.* **AP- 32**:1355-1358.
17. Mitzner, K.M. (1974) *Incremental Length Diffraction Coefficients*, Technical Rept. No. AFAL-TR-73-296 (NTIS No. AD918861).
18. Michaeli, A. (1984) Equivalent edge currents for arbitrary aspects of observation, *IEEE Trans. Antennas Propag.*, **AP-32**:252-258. (1985) **AP- 33**:227.
19. Knott, E.F. (1985) The relationship between Mitzner's ILDC and Michaeli's equivalent currents, *IEEE Trans. Antennas Propag.*, **AP-33**:112-114.
20. Millar, R.F. (1956) An approximate theory of the diffraction of an electromagnetic wave by an aperture in a plane screen, *Proc. IEE*, **103(Pt. C)**:177- 185 (first published as Monograph 152R, 1955).
21. Millar, R.F. (1957) The diffraction of an electromagnetic wave by a circular aperture, *Proc. IEE*, **104(Pt. C)**:87-95 (first published as Monograph 196R, 1956).
22. Millar, R.F. (1957) The diffraction of an electromagnetic wave by a large aperture, *Proc. IEE*, **104(Pt. C)**:240-250 (first published as Monograph 213R, 1956).
23. Ryan, C.E., Jr., and Peters, L., Jr. (1969) Evaluation of edge-diffracted fields including equivalent currents for the caustic regions, *IEEE Trans. Antennas Propag.*, **AP-17**:292-299.
24. Knott, E.F., and Senior, T.B.A. (1974) Comparison of three high-frequency diffraction techniques, *Proc. IEEE*, **62**:1468-1474.

25. Senior, T.B.A., and Uslenghi, P.L.E. (1969) *Electromagnetic and Acoustic Scattering by Simple Shapes*, J.J. Bowman, T.B.A. Senior, and P.L.E. Uslenghi, Eds., Chap. 1, North-Holland, Amsterdam.

26. Whittaker, E.T., and Watson, G.N. (1927) *A Course of Modern Analysis*, Sections 5.31, 5.32, 4th ed., University Press, Cambridge.

27. Michaeli, A. (1986) Elimination of infinities in equivalent edge currents, Part I: Fringe current components, *IEEE Trans. Antennas and Propag.*, AP- 34:912-918.

28. Michaeli, A. (1986) Elimination of infinities in equivalent edge currents, Part II: Physical optics components, *IEEE Trans. Antennas and Propag.*, AP- 34:1034-1037.

29. Bleistein, N. (1984) *Mathematical Methods for Wave Phenomena*, Section 2.7, Academic Press, Orlando.

30. Bowman, J.J., and Senior, T.B.A. (1969) The half-plane, in *Electromagnetic and Acoustic Scattering by Simple Shapes*, J.J. Bowman, T.B.A. Senior, and P.L.E. Uslenghi, Eds., North-Holland, Amsterdam, Chap. 8.

31. Jull, E.V. (1981) *Aperture Antennas and Diffraction Theory*, Institution of Electrical Engineers, London, pp. 80-81.

32. Michaeli, A. (1985) Contribution of a single face to the wedge diffracted field, *IEEE Trans. Antennas and Propag.*, AP-33:221-223.

33. Knott, E.F., Shaeffer, J.F., and Tuley, M.T. (1985) *Radar Cross Section*, Artech House, Dedham, Mass., Chap. 5.

34. Asvestas, J.S., and Kleinman, R.E. (1969) The strip, in *Electromagnetic and Acoustic Scattering by Simple Shapes*, J.J. Bowman, T.B.A. Senior, and P.L.E. Uslenghi, Eds., North-Holland, Amsterdam, Chap. 4.

35. Millar, R.F. (1960) A note on diffraction by an infinite slit, *Can. J. Phys.*, 38:38-47.

36. Bowman, J.J., Senior, T.B.A., and Uslenghi, P.L.E. (1969) *Electromagnetic and Acoustic Scattering by Simple shapes*, North-Holland, Amsterdam, p. 14.

37. Butorin, D.I., and Ufimtsev, P.Ya. (1986) Explict expressions for an acoustic edge wave scattered by an infinitesimal edge element, *Sov. Phys. Acoust.*, 32:283-287.

To prove (4), change the integration variable z′ to z″ = z′ − z, so that the integral becomes

$$F(\bar{\rho},z) = e^{-i\beta z}\int_{-\infty}^{\infty} \frac{e^{i\beta z''}\, e^{ik|\bar{\rho} - \bar{r}''|}}{|\bar{\rho} - \bar{r}''|}\, dz'' = e^{-i\beta z} F_o(\bar{\rho}),\ \beta \equiv k\cos\theta_o. \tag{A1}$$

Because $(\nabla^2 + k^2)\, e^{ik|\bar{r} - \bar{r}'|}/|\bar{r} - \bar{r}'| = -4\pi\,\delta(\bar{r} - \bar{r}')$, taking the Laplacian of (A1) shows that $F_o(\bar{\rho})$ obeys the scalar wave equation

$$\nabla_t^2 F_o + (k^2 - \beta^2)F_o = -4\pi\,\delta(\bar{\rho} - \bar{\rho}'). \tag{A2}$$

$$\nabla_t^2 \equiv \nabla^2 - \frac{\partial^2}{\partial z^2}$$

Letting $\rho \to \infty$ in (A1), one sees that $F_o(\bar{\rho})$ satisfies the radiation condition

$$F_o(\bar{\rho}) \overset{\rho\to\infty}{=} O\left(\frac{e^{ik\rho}}{\sqrt{\rho}}\right). \tag{A3}$$

Thus, (A2) has the well-known unique solution

$$F_o = i\pi\, H_o^{(1)}\left(\sqrt{k^2 - \beta^2}\, |\bar{\rho} - \bar{\rho}'|\right). \tag{A4}$$

*U.S. GOVERNMENT PRINTING OFFICE: 1989-600-000/00006

MISSION of Rome Air Development Center

RADC plans and executes research, development, test and selected acquisition programs in support of Command, Control, Communications and Intelligence (C^3I) activities. Technical and engineering support within areas of competence is provided to ESD Program Offices (POs) and other ESD elements to perform effective acquisition of C^3I systems. The areas of technical competence include communications, command and control, battle management, information processing, surveillance sensors, intelligence data collection and handling, solid state sciences, electromagnetics, and propagation, and electronic, maintainability, and compatibility.